

# Simulating Supersonic Parachutes For Mars Entry, Descent & Landing

Supercomputing Conference  
Dallas, TX Nov 13-18, 2022



*Francois Cadieux*

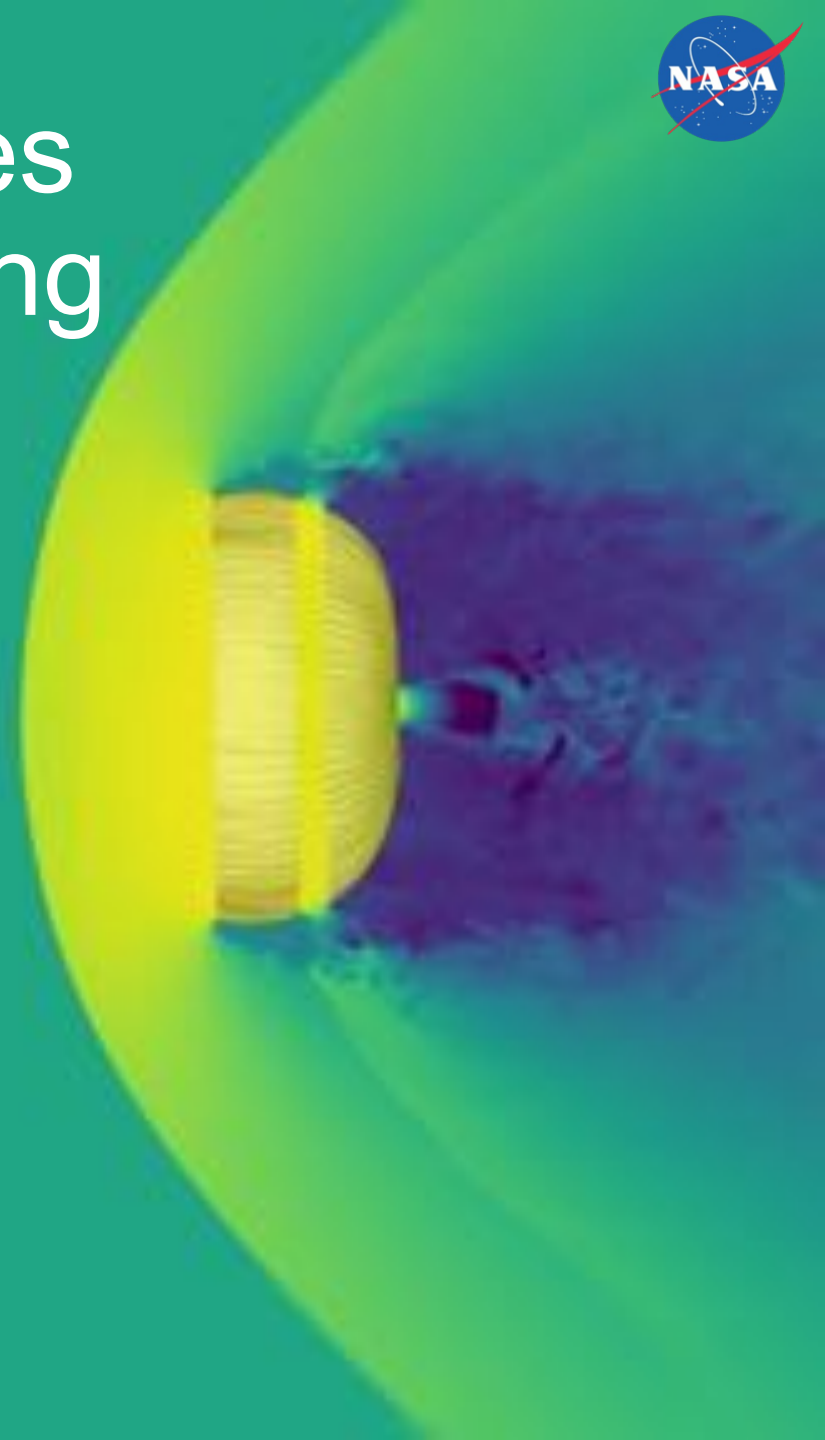
*Jordan Angel*

*Michael Barad*

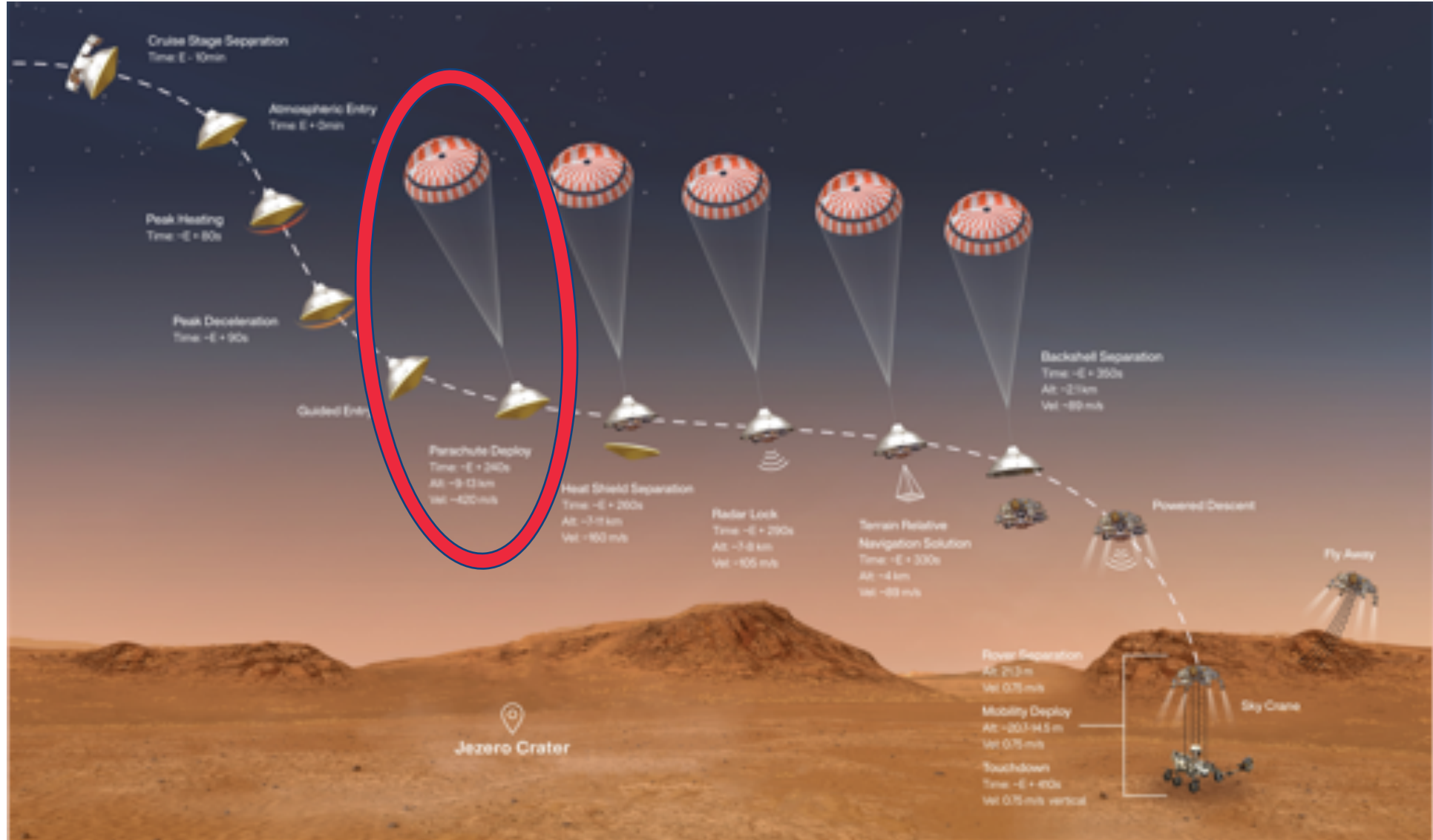
*Cetin Kiris*

*with work done by Jonathan Boustani*

POC: [francois.cadieux@nasa.gov](mailto:francois.cadieux@nasa.gov)



# Context: Perseverance Rover's EDL Profile



# Motivation: Low Density Supersonic Decelerator



- Low density supersonic decelerator (LDSD) project aimed to test two novel technologies:
  - an inflatable decelerator
  - *a new Disksail parachute design* [1]
- Disksail parachute showed signs of damage early on during its inflation and ultimately was ripped apart
- Cause of failure still poorly understood today
- Leading hypothesis is that the new Disksail design itself caused more severe stresses than seen in previous disk-gap-band (DGB) parachutes [2]:
  - its larger shoulder region may have pulled the disk portion of the canopy flat earlier in the inflation process, causing the fabric to tear under the increased load



NASA JPL: <https://youtu.be/9yRWWhu0UGYw?t=74>

[1] Gallon, J., Witkowski, A., Clark, I. G., Rivellini, T., and Adams, D. S., "Low density supersonic decelerator parachute decelerator system," AIAA Aerodynamic Decelerator Systems (ADS) Conference, 2013, p. 1329

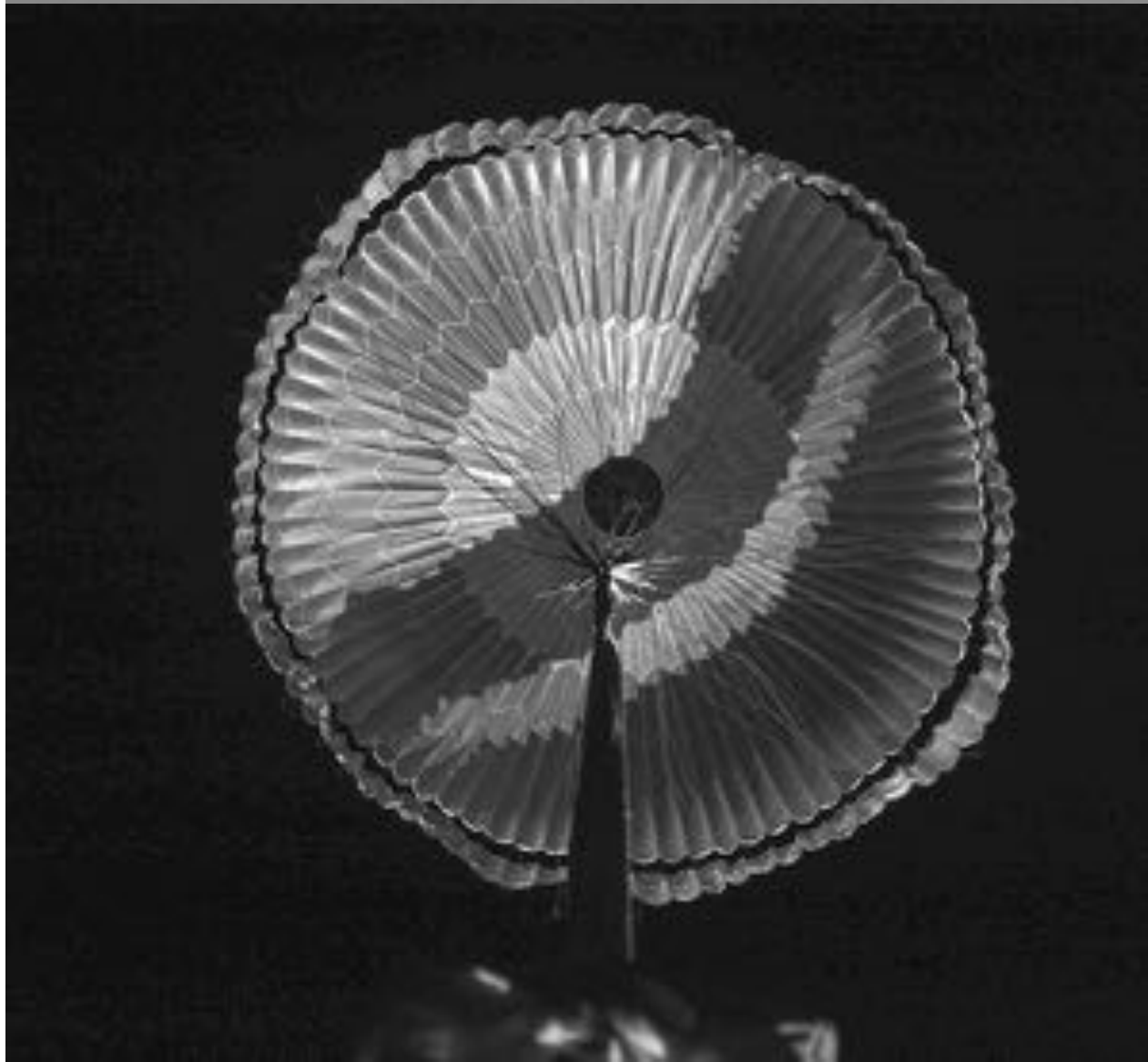
[2] Clark, I. G., Gallon, J. C., and Witkowski, A., "Parachute Decelerator System Performance During the Low Density Supersonic Decelerator Program's First Supersonic Flight Dynamics Test," 23rd AIAA Aerodynamic Decelerator Systems Technology Conference, 2015, p. 2130

# ASPIRE: Testing a Parachute for Mars



Credits: NASA/JPL-Caltech

<https://www.nasa.gov/feature/jpl/third-aspire-test-confirms-mars-2020-parachute-a-go>



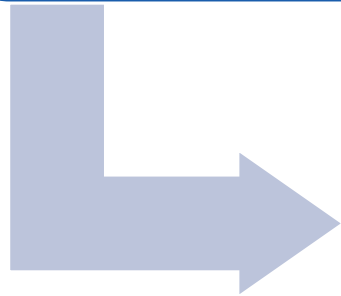
NASA/JPL:

<https://youtu.be/AcAgnQ9K7UY>

# Problem Description

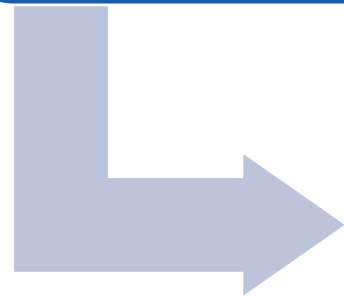
LDSD  
Parachute  
Failure

- LDSD project demonstrated that NASA & JPL could not predict the failure of a new parachute system design, or establish with confidence the cause of failure after the fact



ASPIRE:  
3 Successful  
Tests

- The Advanced Supersonic Parachute Inflation Research Experiments (ASPIRE) tested parachutes intended for Mars landings (e.g. Perseverance) in supersonic conditions in the upper earth atmosphere



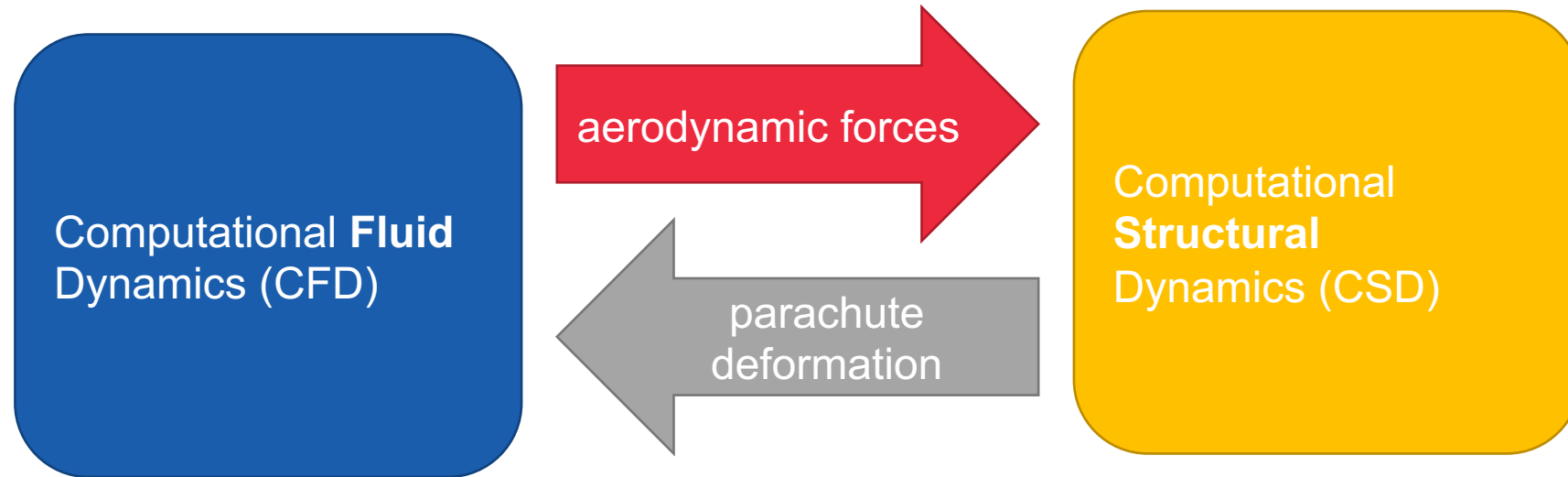
Fluid-Structure  
Interaction  
(FSI)  
Simulations

- Predictive computational modeling of the parachute system as it is deployed could provide insight at much lower cost and mitigate risk of failures like the LDSD

# Research Objectives



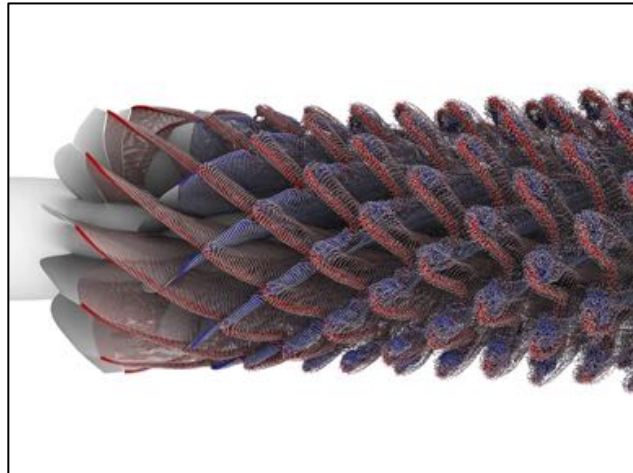
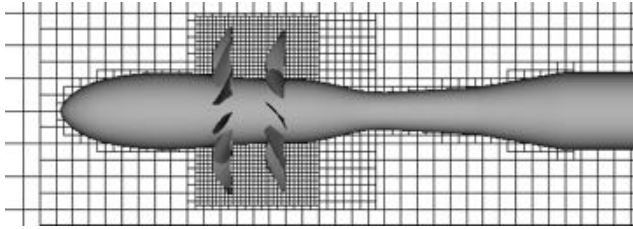
- Develop FSI capability to simulate supersonic parachute inflation



- Validate FSI predictions with ASPIRE test measurements
- Leverage FSI capability to help in design of next generation of parachutes using best practices established for ASPIRE

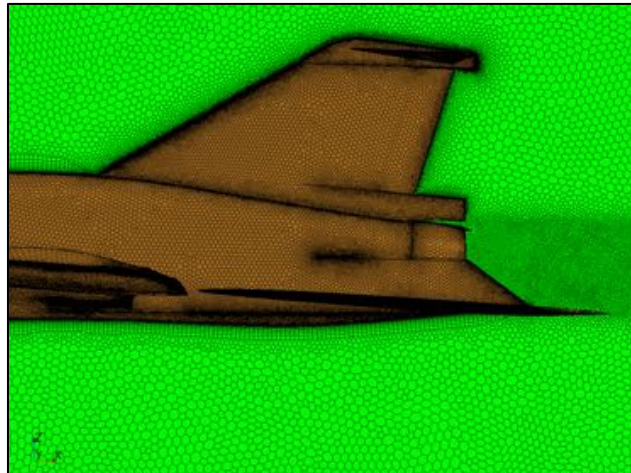
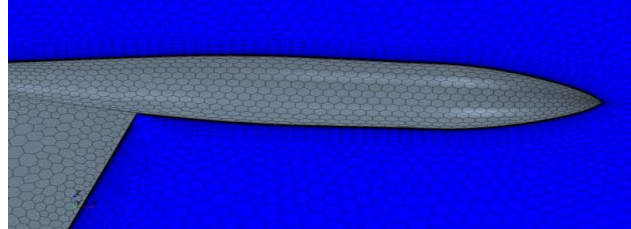
# Choosing a CFD Grid Paradigm

## Structured Cartesian AMR



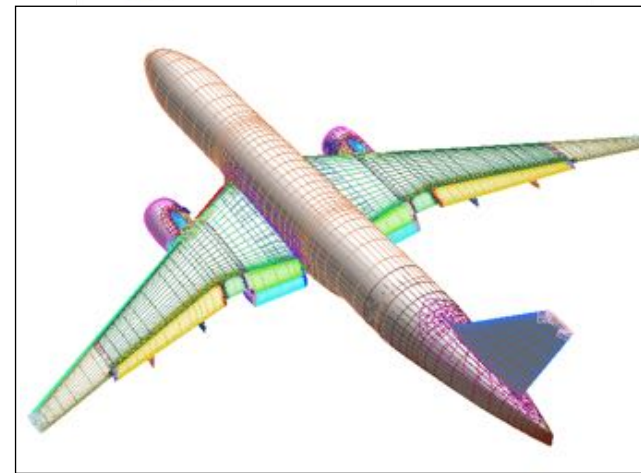
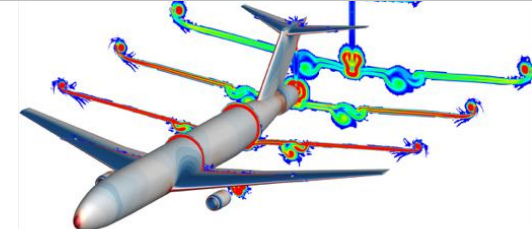
- Essentially no manual grid generation
- Highly efficient Structured Adaptive Mesh Refinement (AMR)
- Low computational cost
- Reliable higher order methods
- Non-body fitted → Resolution of boundary layers challenging

## Unstructured Arbitrary Polyhedral



- Partially automated grid generation
- Body fitted grids
- Grid quality can be challenging
- High computational cost
- Higher order methods yet to fully mature

## Structured Curvilinear

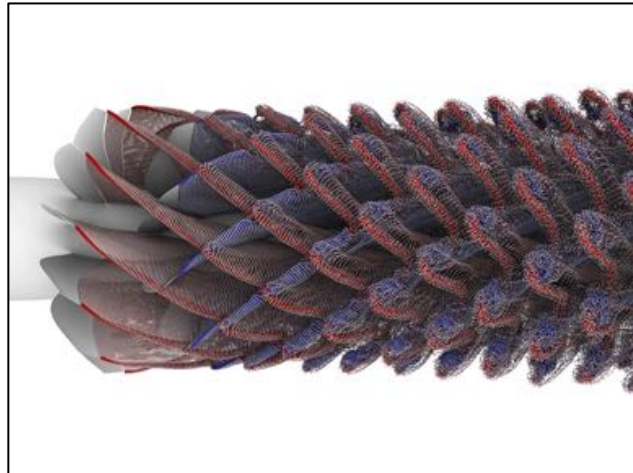
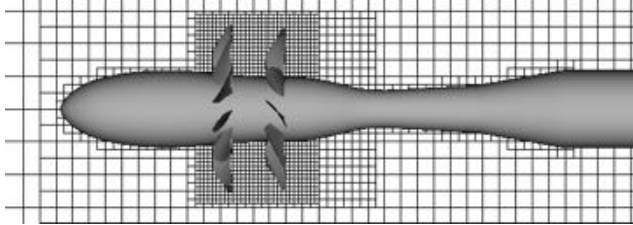


- High quality body fitted grids
- Low computational cost
- Reliable higher order methods
- Grid generation largely manual and time consuming

# Choosing a CFD Grid Paradigm



## Structured Cartesian AMR

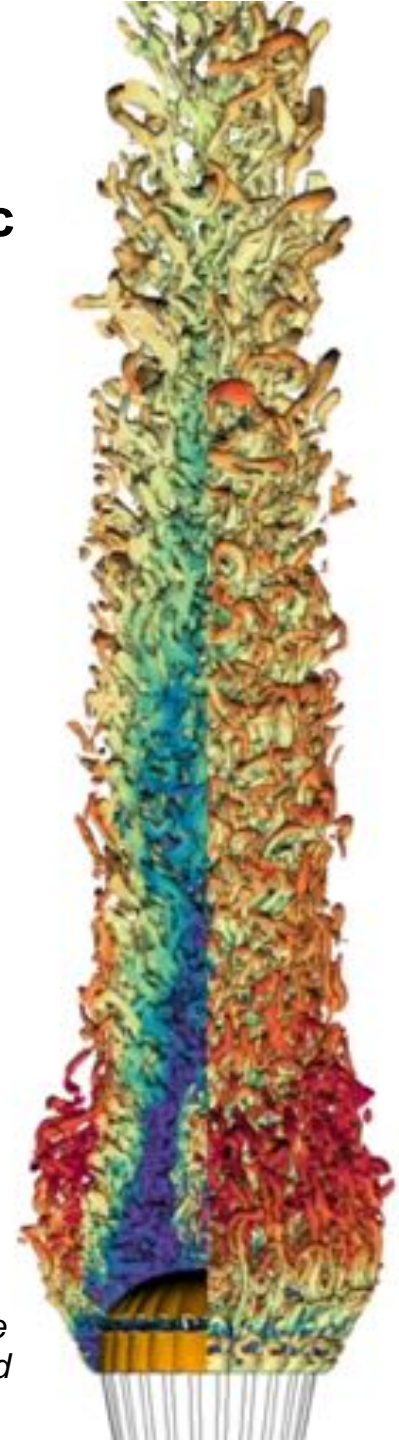


- Essentially no manual grid generation
- Highly efficient Structured Adaptive Mesh Refinement (AMR)
- Low computational cost
- Reliable higher order methods
- **Non-body fitted → Resolution of boundary layers challenging**

## Requirements for Simulating Supersonic Parachute Inflation Process:

- ✓ Simulate inherently transient phenomenon in a time-accurate fashion efficiently
- ✓ Resolve moving bow shocks, payload and canopy wake
- ✓ Adapt grid to *large* deformations of parachute during inflation
- ✓ Thin attached boundary layers do not play a critical role in determining the inflation dynamics of the parachute: it is driven by pressure effects and not skin friction

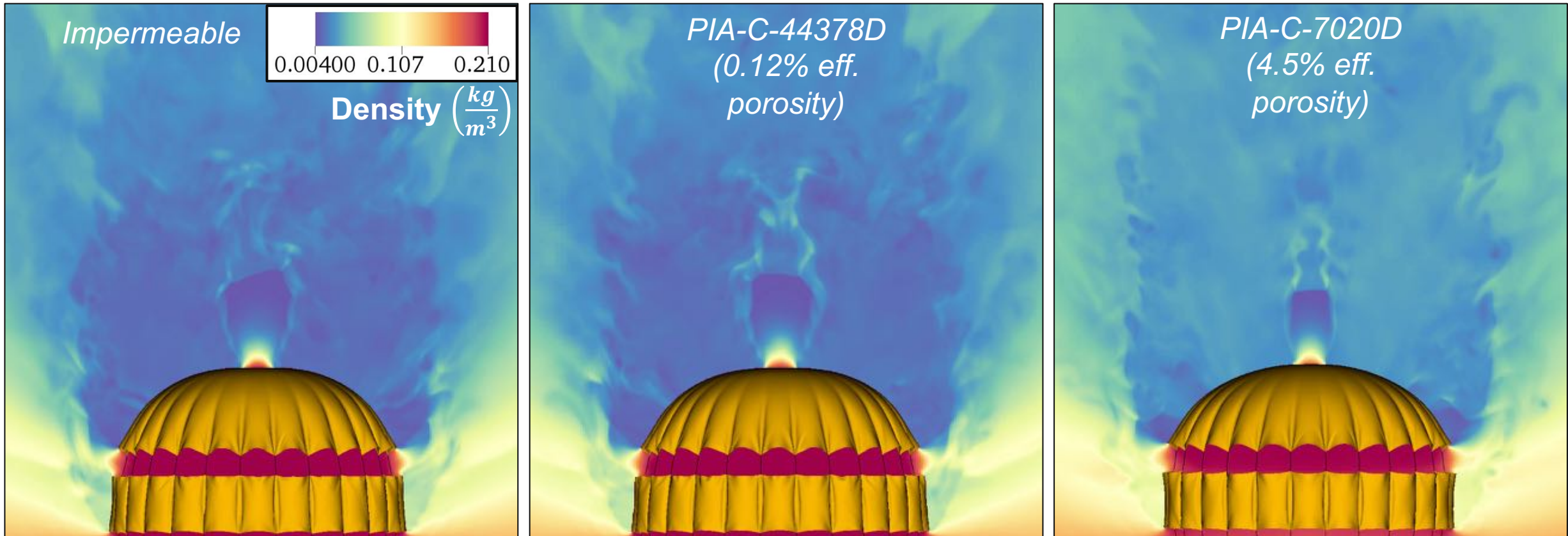
*Isocontours of Q-criterion colored by Mach number where blue is lower and red is higher.*





# Modeling Parachute Broadcloth Porosity

- Obtain closed-form solution to equations describing flow through porous material
- Apply solution as a jump conditions in CFD to avoid requirement to resolve flow through the parachute fabric's thickness ( $7.62 \times 10^{-6} \text{m}$ )

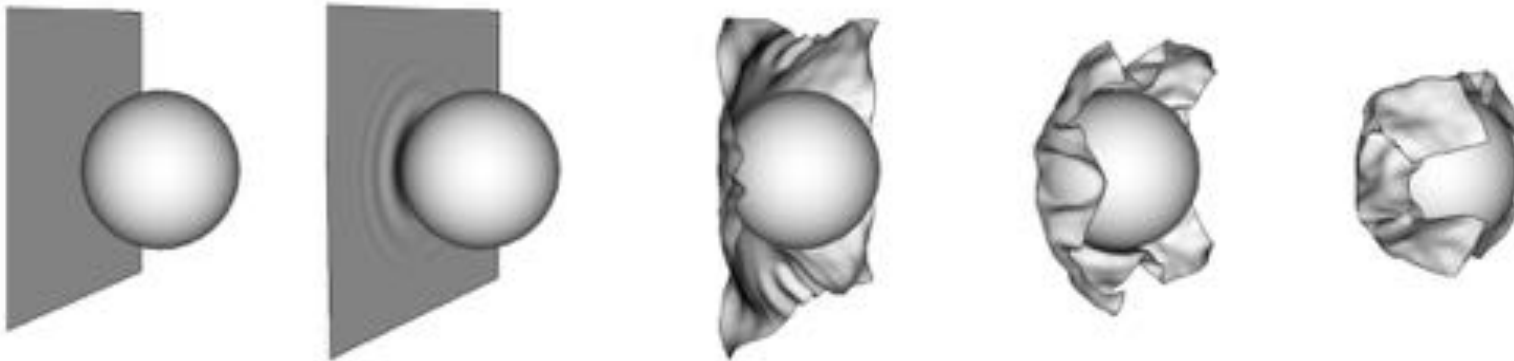


- Higher porosity  $\rightarrow$  weaker recirculation  $\rightarrow$  more stable dynamics

# Identifying and Enforcing Contact Mechanics

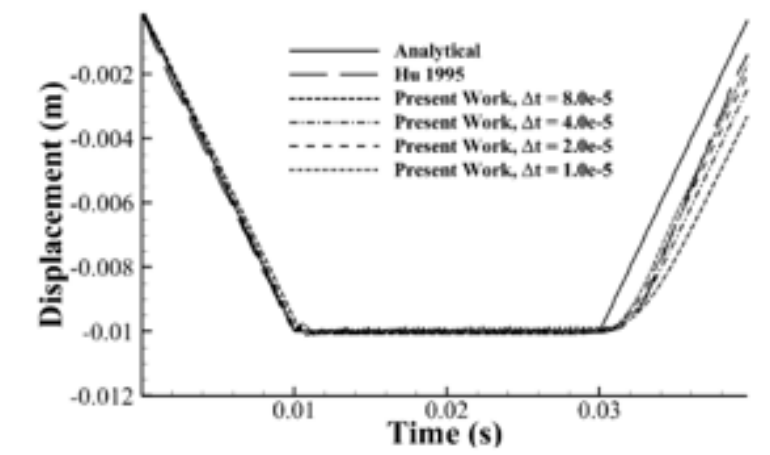
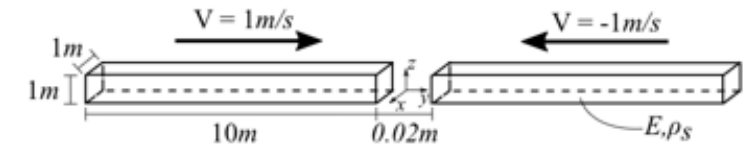


- Before communicating aerodynamic forces to structural dynamics, identify triangles on surface who could soon come into contact by checking if ray traced from one triangle face pierces another within a given distance
- If a pair of triangles have velocities that will close the gap between them and cause contact to occur, we add a momentum force that models an elastic collision: this allows contact without surface (self-) intersections



Snapshots in time of a test case demonstrating the contact identification and enforcement method

Setup and results from a canonical 1D contact problem



# Contact Demonstration For Parachute Inflation

It's not yet computational tractable to simulate the ASPIRE parachute as it rips out from its bag, so we start from a folded shape with 40% of its flat diameter, in which the 80 gores and 40 suspension lines are arranged like an accordion in 40 peaks and valleys

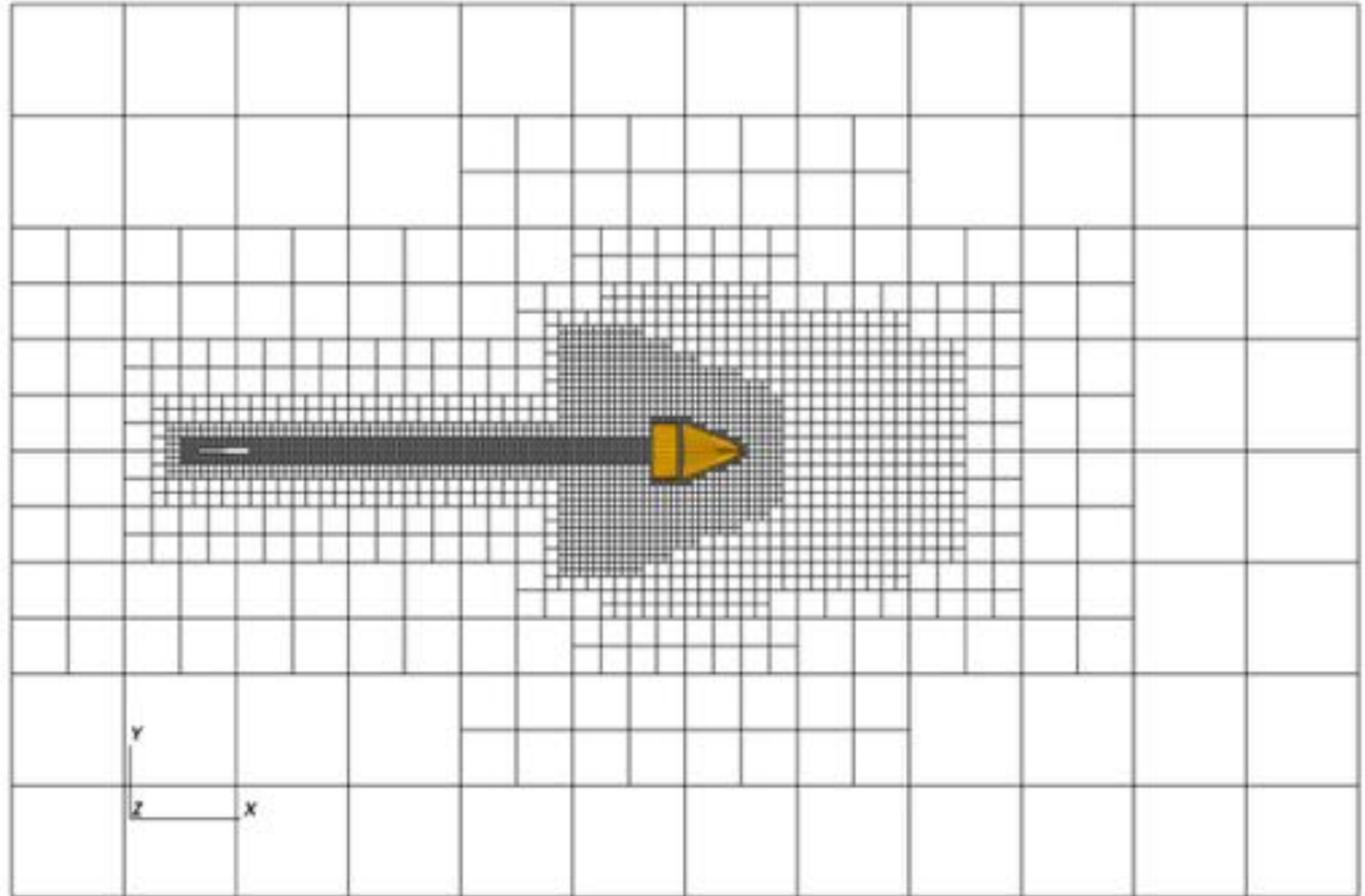


*Animation showing parachute inflation from a structural-only simulation to evaluate the contact identification and enforcement algorithm. The CSD solver is exposed to a constant surface normal force.*

# Cartesian AMR Grid For ASPIRE SR01 FSI

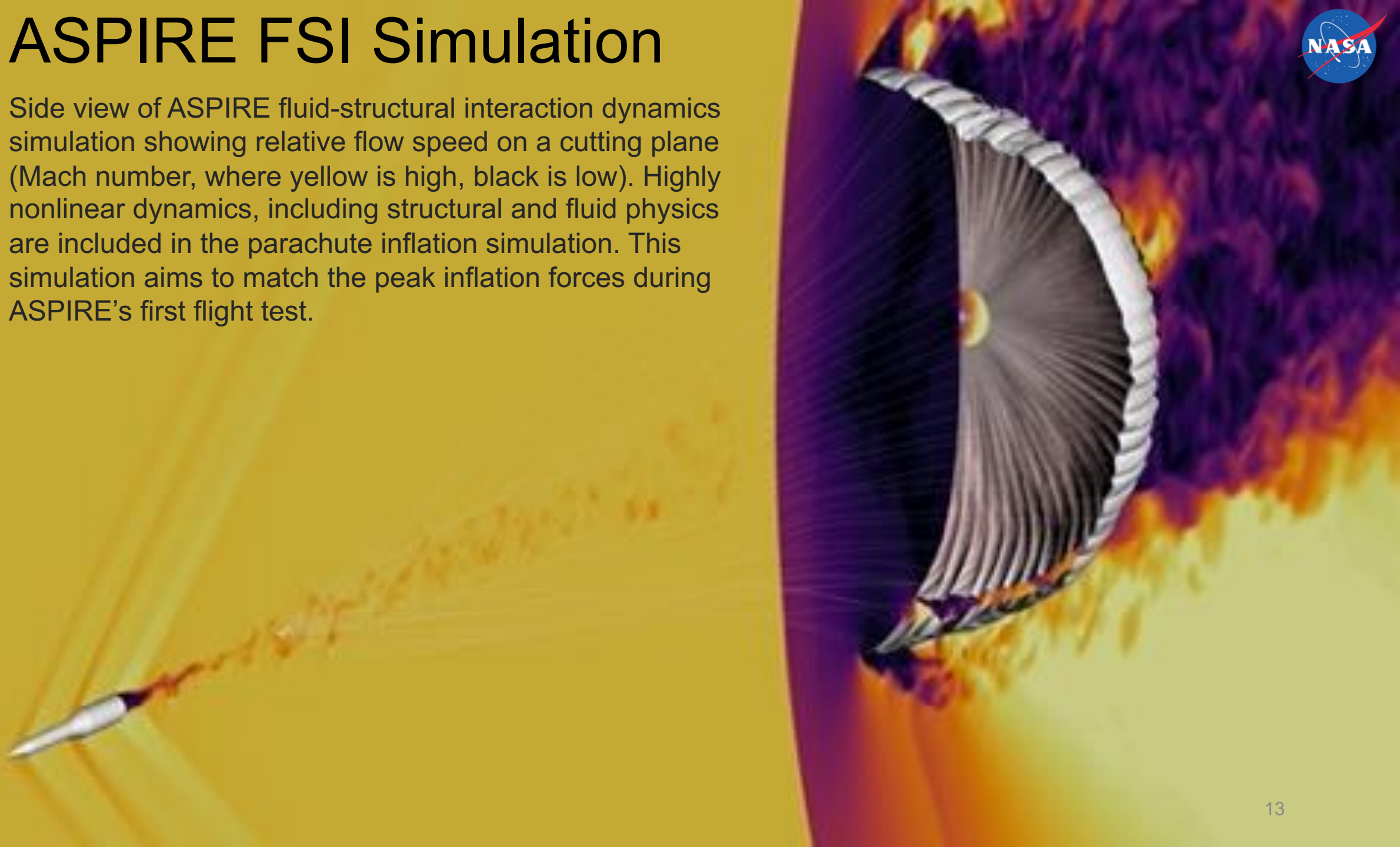


- Each box contain  $16^3$  cells
- AMR is used to ensure parachute canopy is surrounded by fine grid cells during inflation
- Finest cells have  $\Delta x = 2.4cm$  , and every subsequent level is twice larger in all directions



# ASPIRE FSI Simulation

Side view of ASPIRE fluid-structural interaction dynamics simulation showing relative flow speed on a cutting plane (Mach number, where yellow is high, black is low). Highly nonlinear dynamics, including structural and fluid physics are included in the parachute inflation simulation. This simulation aims to match the peak inflation forces during ASPIRE's first flight test.



# Qualitative Comparison To ASPIRE SR01



*Credits: NASA/JPL-Caltech*

<https://www.nasa.gov/feature/jpl/third-aspire-test-confirms-mars-2020-parachute-a-go>

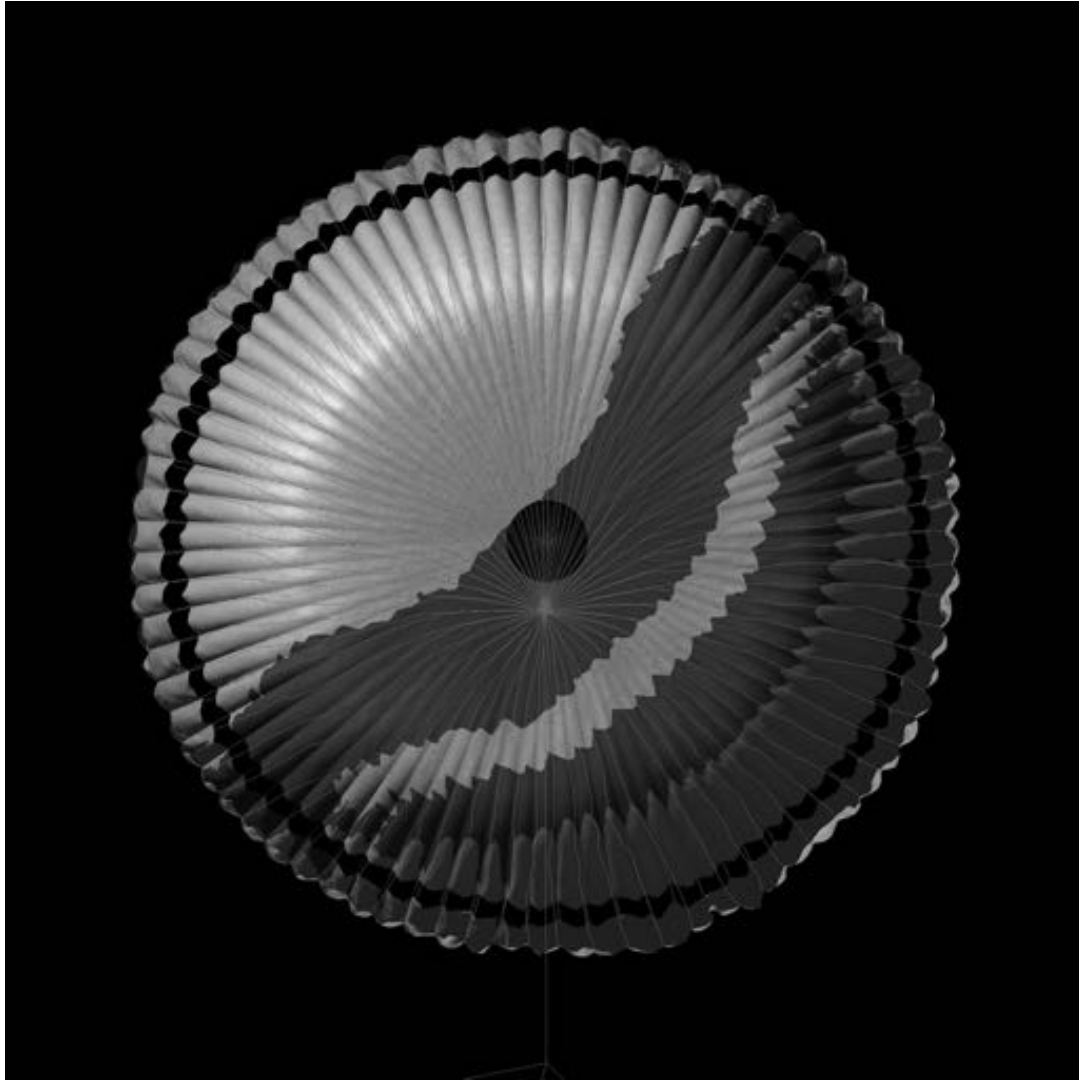
Unsteady view of the parachute FSI from the attachment point (hyperwall). This view is designed to match the camera view taken during the actual ASPIRE SR01 test flight (above). Geometrically nonlinear structural dynamics can be seen as the parachute and lines undergo large unsteady deformations.

# Qualitative Comparison To ASPIRE SR01



Credits: NASA/JPL-Caltech

<https://www.nasa.gov/feature/jpl/third-aspire-test-confirms-mars-2020-parachute-a-go>



LAVA FSI



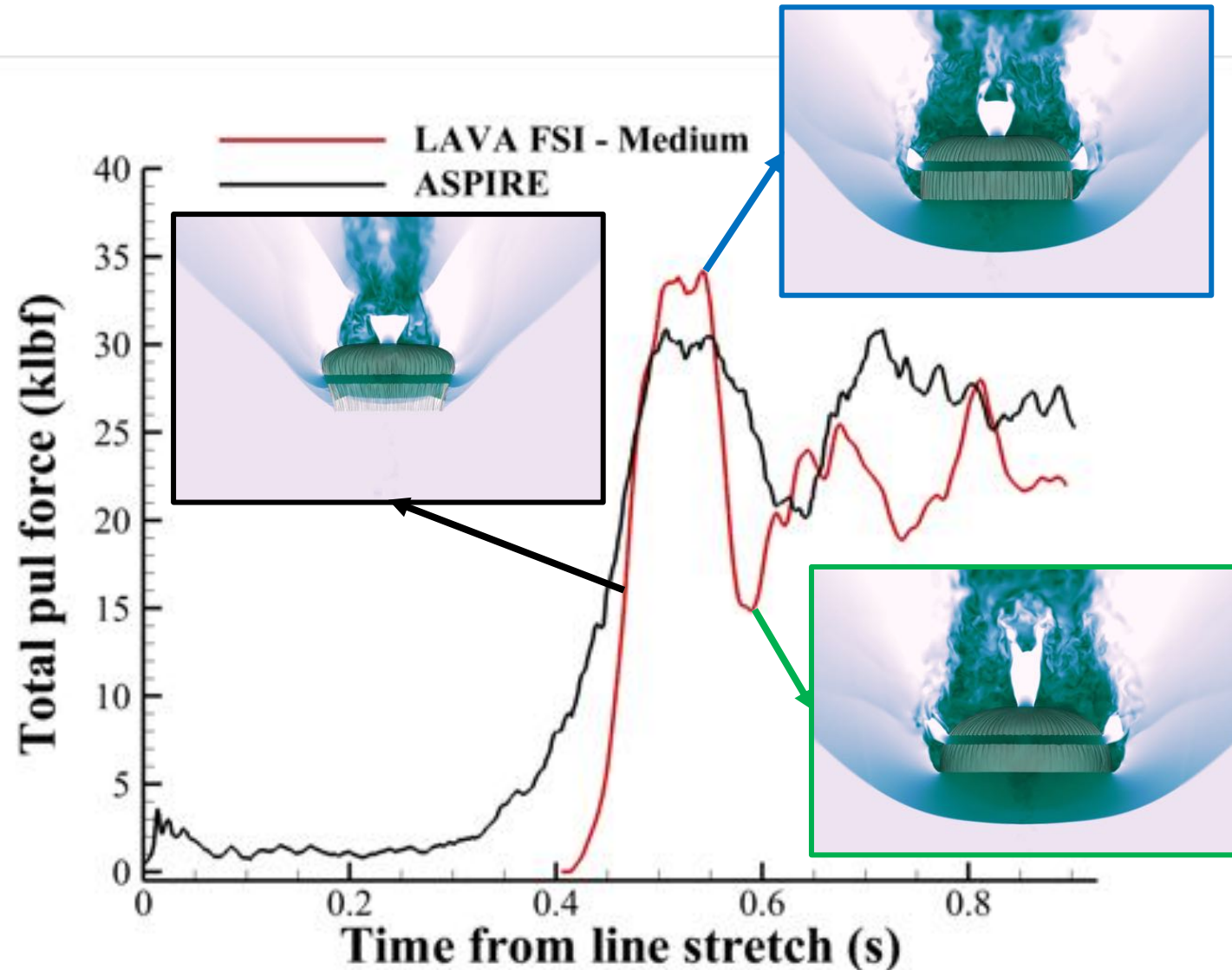
ASPIRE SR01 Picture

Comparison of ASPIRE SR01 canopy shape with 3D shadows rendered

# Validation of ASPIRE SR01 FSI Simulation



- ASPIRE payload had 3 load pins to measure the tension in the triple bridle as a function of time with a measurement uncertainty of about 6% of peak load ( $\pm 1.82$  klbf)
- FSI simulation recorded the restoring force in the elements of each bridle to perform as close to apples-to-apples comparison of total pull force
- FSI shows qualitative behavior consistent with ASPIRE test
- FSI inflates faster and overpredicts inflation peak by  $\sim 10\%$
- FSI underpredicts trough and rebound peak by  $\sim 20\%$







# Possible Sources of Error

## 1. Numerical Error

- Occurs whenever the spatio-temporal scales of motion in the problem simulated are not sufficiently resolved
- Reducing this error is a matter of reducing  $(\Delta t, \Delta x)$  while still integrating a large enough time interval to capture phenomenon of interest
- Grid convergence studies can provide an estimate of converged value of a quantity of interest (e.g. pull-force) and a measure of uncertainty related to numerical error

## 2. Modeling Error

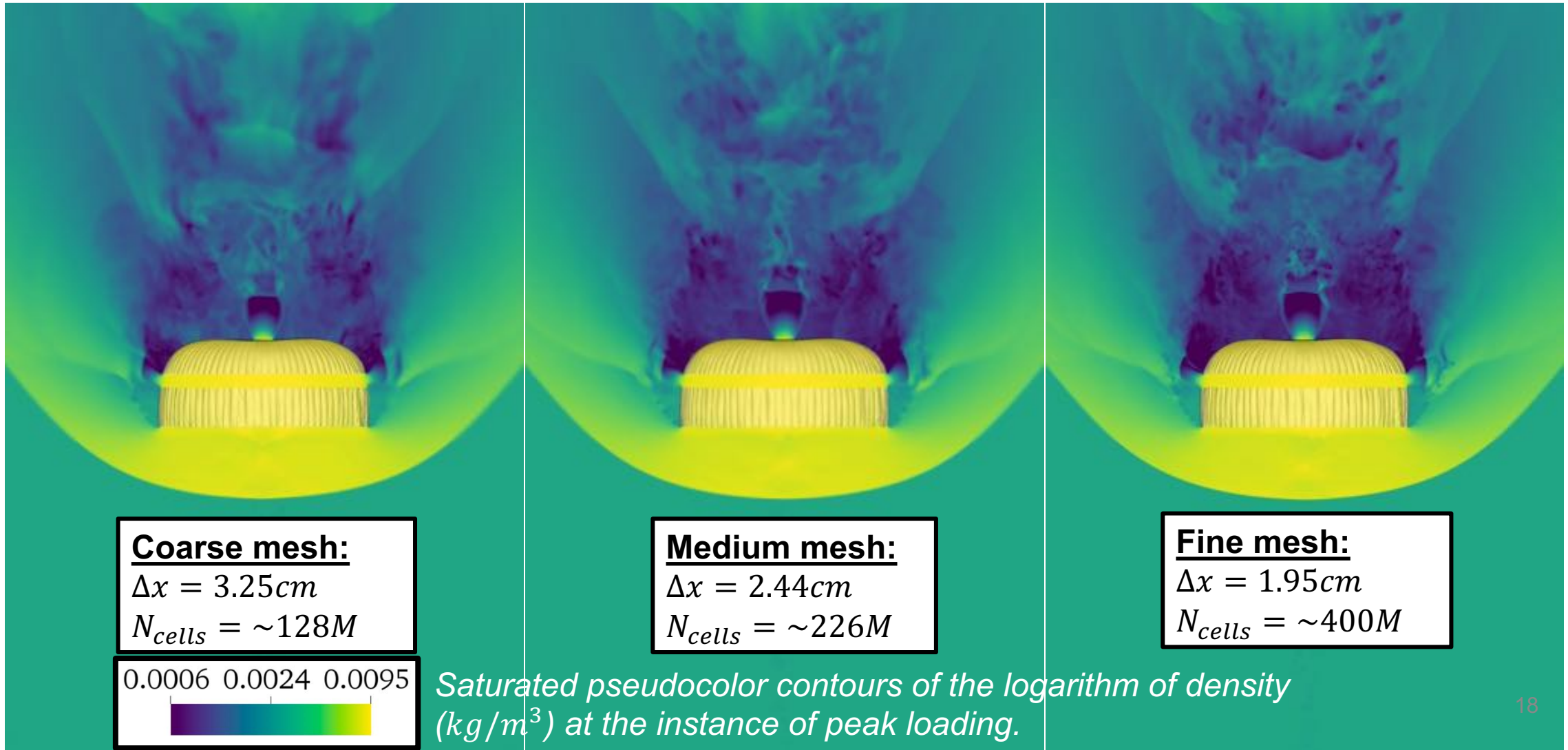
- Modeling error occurs every time a simplifying assumption is made that does not fully represent the underlying physics
- Bounding this error requires obtaining the degree of sensitivity of quantities of interest to assumptions made by either removing or changing them one at a time
- Expert knowledge of the problem is often required to identify the assumptions that are most likely to cause significant changes in the quantity of interest

Assessing numerical and modeling errors are both computationally costly!  
We will only assess numerical errors in this presentation.

# ASPIRE FSI Grid Convergence Study

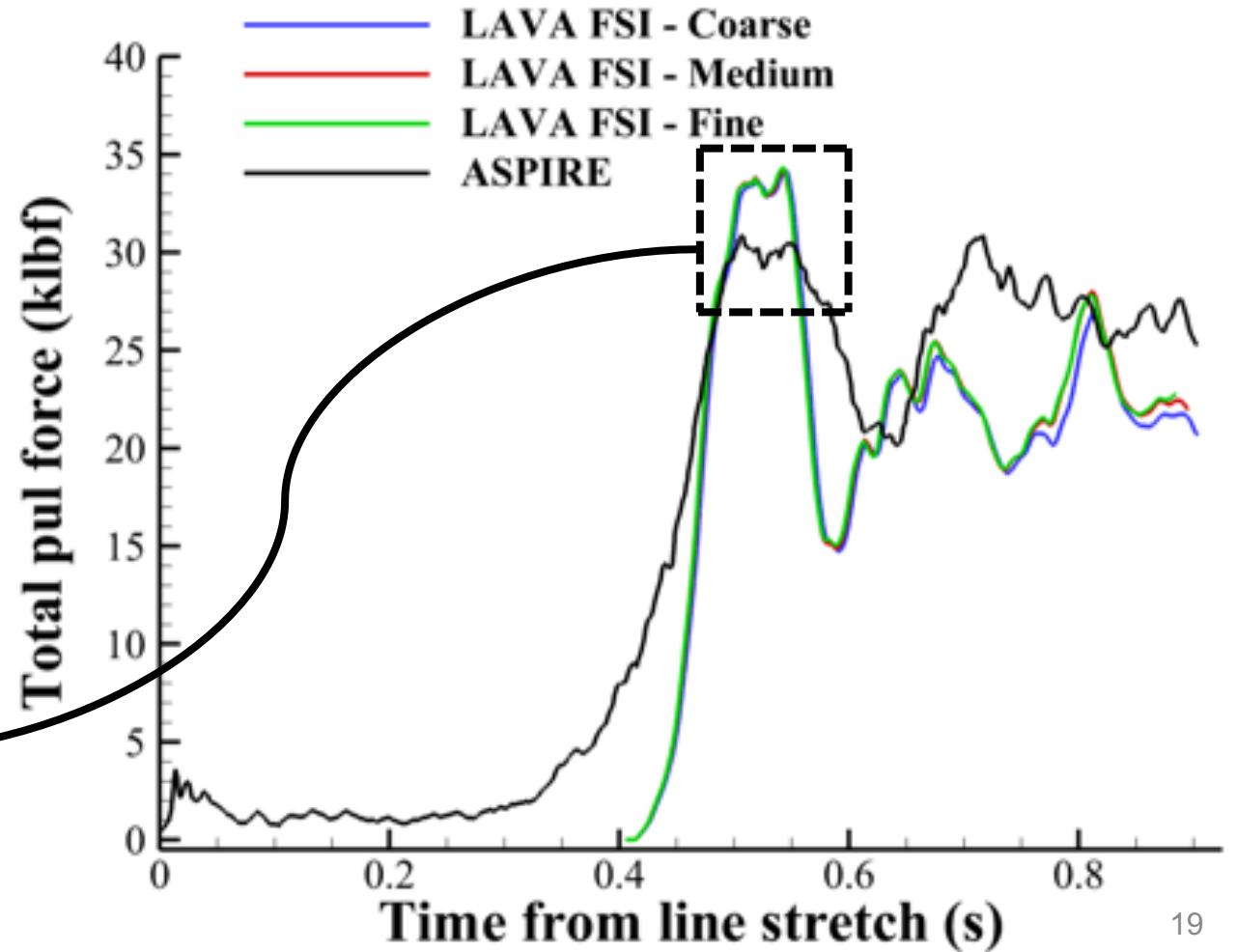
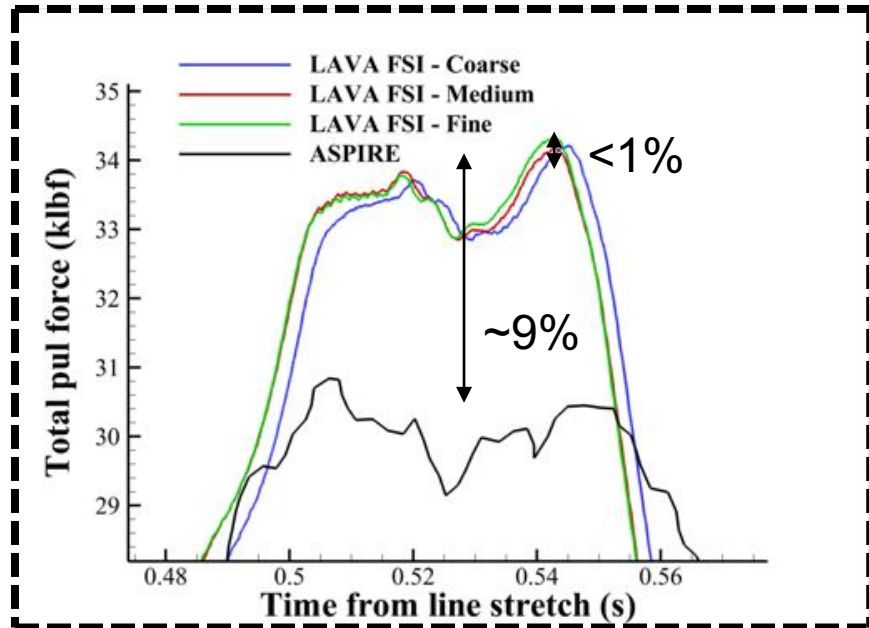


- In order to ensure differences between FSI and flight test are not due to CFD resolution, we coarsen by  $2^{1/3}$  and refine by  $1/2^{1/3}$  every cell in the domain and perform two additional simulations



# ASPIRE FSI Grid Convergence Results

- Observed clear convergence behavior: Medium and Fine grid are on top of each other
- All 3 CFD grid resolutions predict inflation peak load within 1% of each other



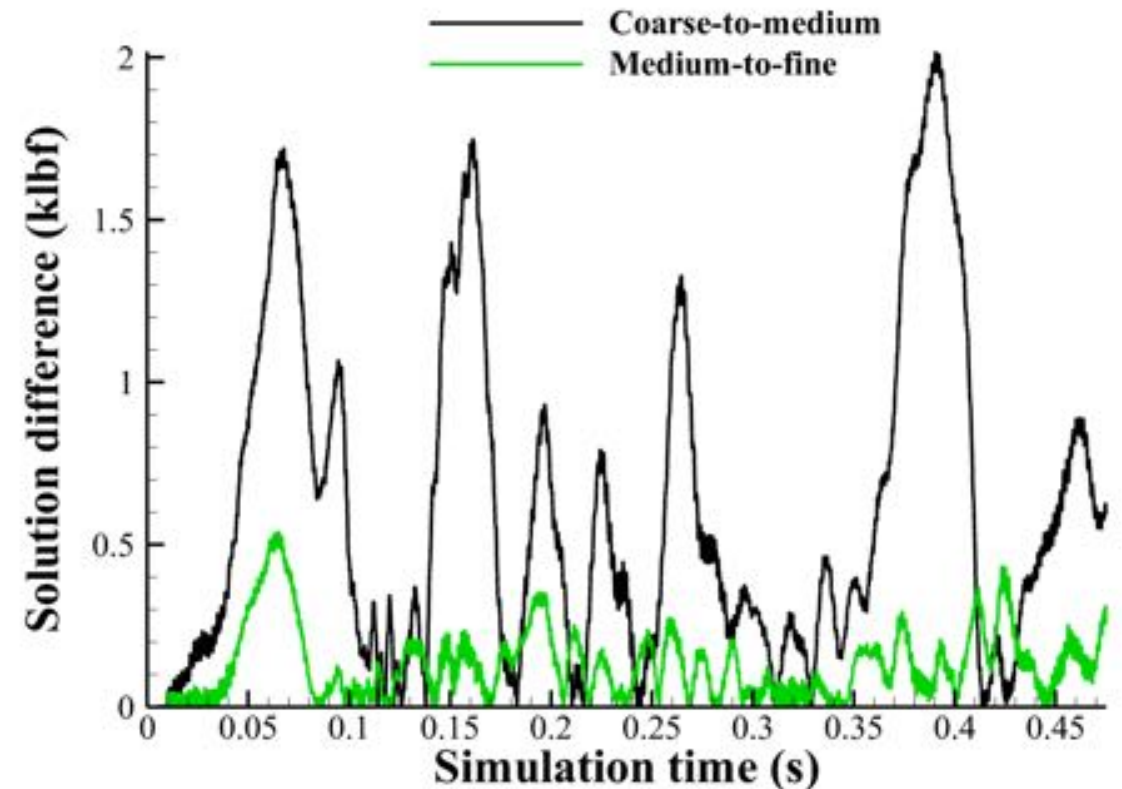
# ASPIRE FSI Grid Convergence Results



- Interpolate coarse and medium pull-force time curve onto fine and use mean difference from coarse-to-medium and medium-to-fine to compute a convergence rate
- CFD and CSD time integrator are 2<sup>nd</sup> order accurate, so obtaining 3<sup>rd</sup> order convergence indicates that spatial error from high-order shock capturing scheme dominates

For the available time interval

| Error Norm | Convergence Rate |
|------------|------------------|
| L-1        | 2.99             |
| L-2        | 3.01             |
| L-∞        | 2.57             |



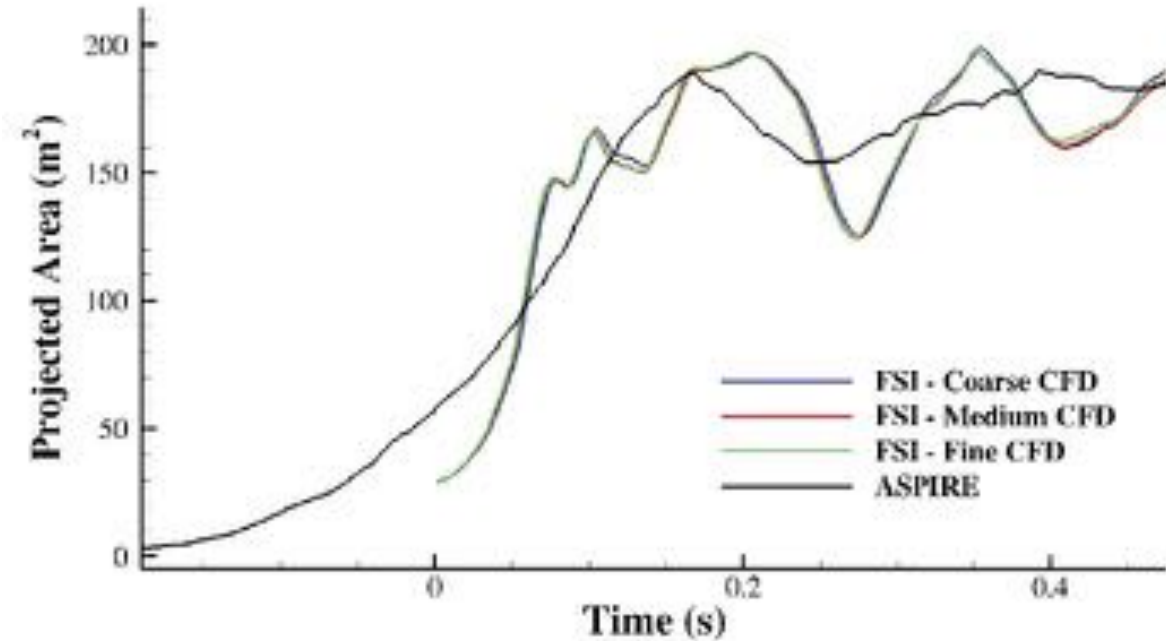
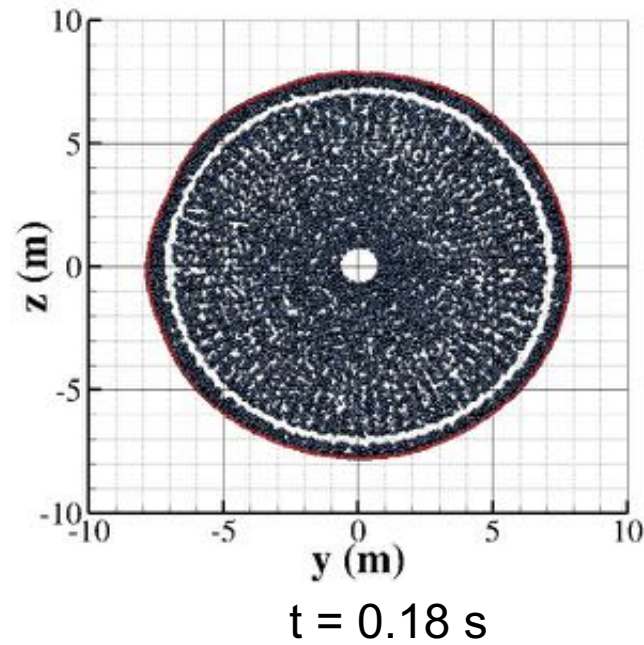
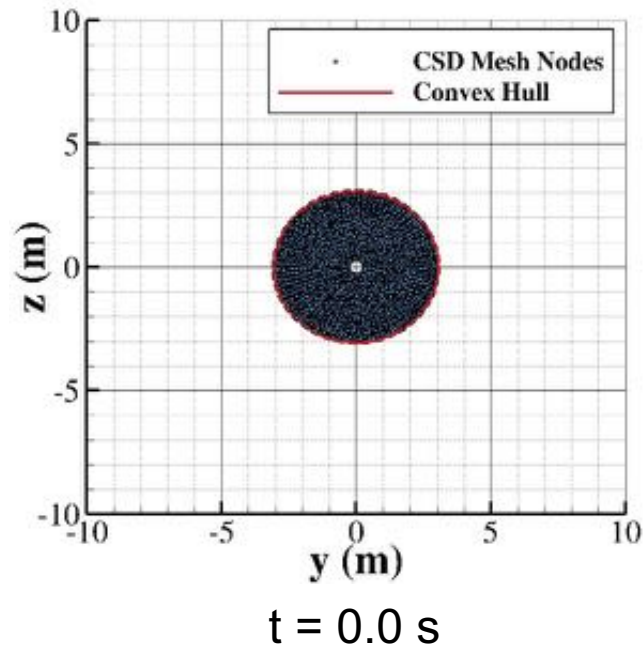
For more grid convergence metrics, please refer to [3]

[3] Boustani, J., Cadieux, F., Kenway, G. K., Barad, M. F., Kiris, C. C., and Brehm, C., "Fluid-structure interaction simulations of the ASPIRE SR01 supersonic parachute flight test," *Aerospace Science and Technology*, 2022, p. 107596

# ASPIRE FSI Grid Convergence Results

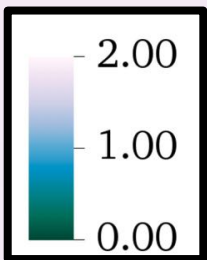


- We can compute projected area in a similar fashion to ASPIRE test
- All 3 CFD grid resolutions predict inflation peak projected area within 1% of each other
- FSI shows faster inflation and deeper rebound than measured during ASPIRE SR01



# ASPIRE FSI Structural Grid Refinement

- In order to ensure differences between FSI and flight test are not due to insufficient structural grid resolution, we refine by  $1/2^{1/3}$  every end on the parachute surface and perform another simulation (1.26M  $\rightarrow$  2.22M DOF)

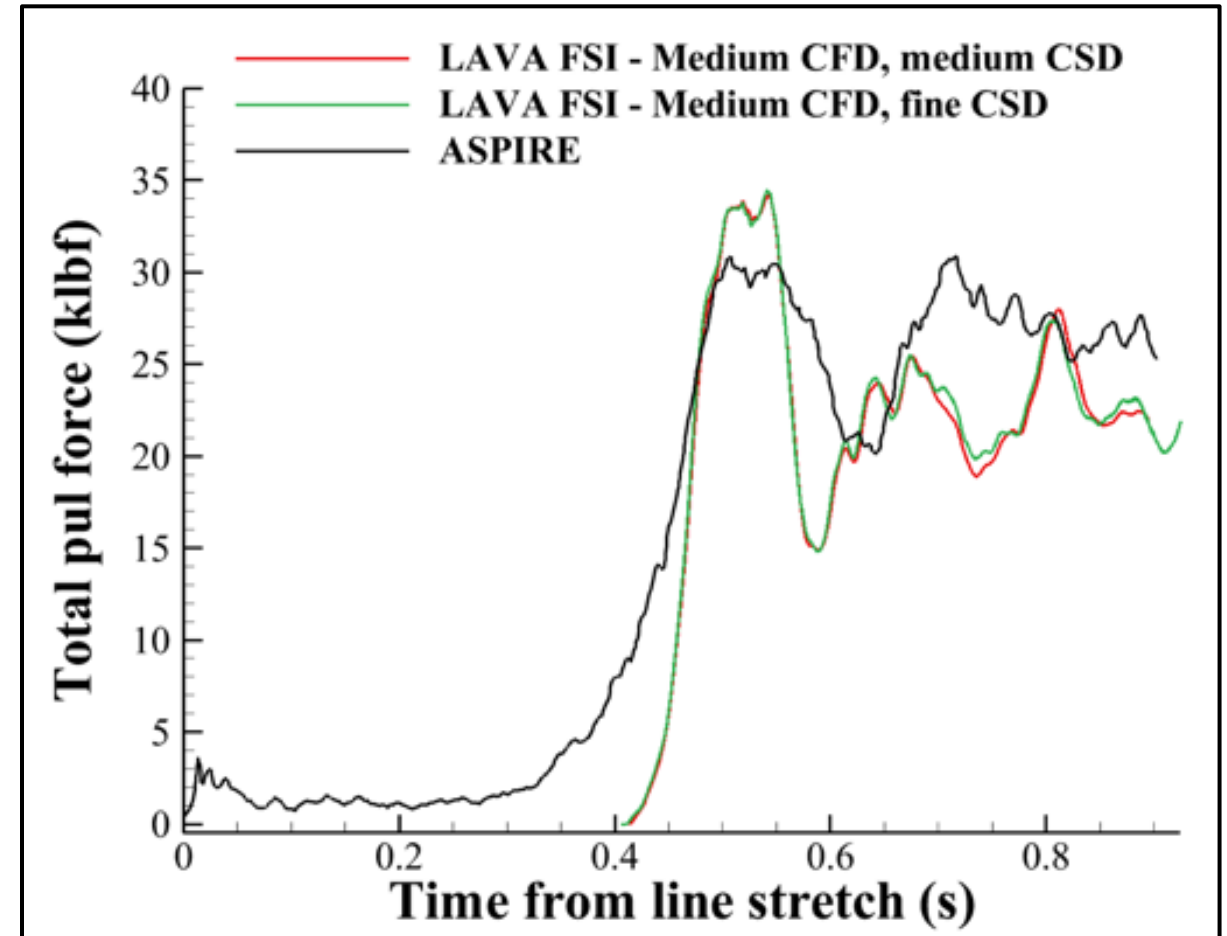


*Saturated pseudocolor contours of Mach number shown on a cut-plane through the center of the domain for a medium CFD - fine CSD simulation of ASPIRE SR01.*

# ASPIRE FSI Structural Grid Refinement



- Results indicate <math><1\%</math> sensitivity for inflation peak, and only minor deviations in the post-rebound phase
- From CFD grid convergence study and structural refinement results, we can eliminate both spatial discretizations as the primary source of the discrepancy between FSI and ASPIRE test data



# Computational Cost of FSI Simulations



## Computational Cost

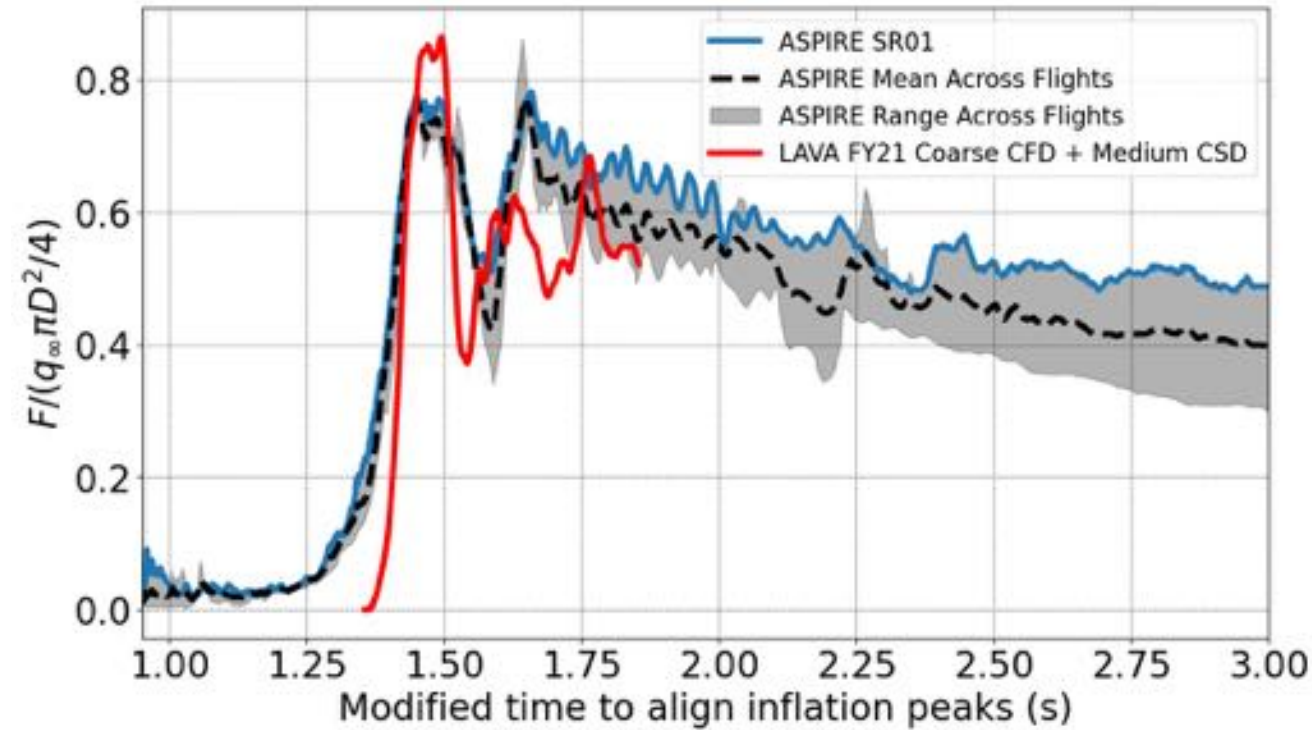
| CFD Grid Cells | CSD Degrees of Freedom | Number of Cascade Lake CPU Cores | Wall time (hours) | Core-hours x10 <sup>3</sup> |
|----------------|------------------------|----------------------------------|-------------------|-----------------------------|
| Coarse (~128M) | Medium (1.26M)         | 1600                             | 32                | 51.2                        |
| Medium (~226M) | Medium (1.26M)         | 960                              | 67                | 64.3                        |
| Fine (~400M)   | Medium (1.26M)         | 2400                             | 70                | 168.0                       |
| Medium (~226M) | Fine (2.22M)           | 2400                             | 58                | 139.2                       |

- Turnaround time on coarse mesh is just over 24 hours: could enable system level studies
- Computational cost doesn't scale linearly: current bottleneck is not solving the multi-physics equations themselves, but the process of tracking the parachute's deformation and applying boundary conditions



# A Note on Flight Test Uncertainty

- Measurement uncertainty is not the same as uncertainty stemming from repeated tests
- ASPIRE project conducted 3 tests: SR01, SR02, and SR03:
  - Each test saw differences in parachute diameter, materials, construction, and release mechanism, along with significant increases in dynamic pressure when released
- We can gain information about flight test repeatability if we non-dimensionalize the pull-force by parachute area and dynamic pressure



| Non-Dimensional Drag Force | ASPIRE Average Across Flights | LAVA FSI Predictions FY21 Coarse CFD + Medium CSD Mesh | ASPIRE Percent Variation Across Flights (+/-) | Percent Difference Btw LAVA and ASPIRE Average |
|----------------------------|-------------------------------|--|---|--|
| Inflation Peak             | 0.773                         | 0.865  | 3.42  | +11.9  |
| Rebound Peak               | 0.798                         | 0.624  | 14.93   | -21.8  |
| Trough                     | 0.409                         | 0.372  | 42.10   | -9.1   |



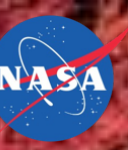
# Sources of Uncertainty in FSI

As demonstrated by CFD and CSD grid refinement studies, FSI simulations are repeatable and show little discretization related uncertainty. Flight tests non-dimensional inflation peaks are also highly repeatable and show little flight-to-flight variation.

We conclude that the discrepancy in predicted pull-force stems from **modeling errors**:

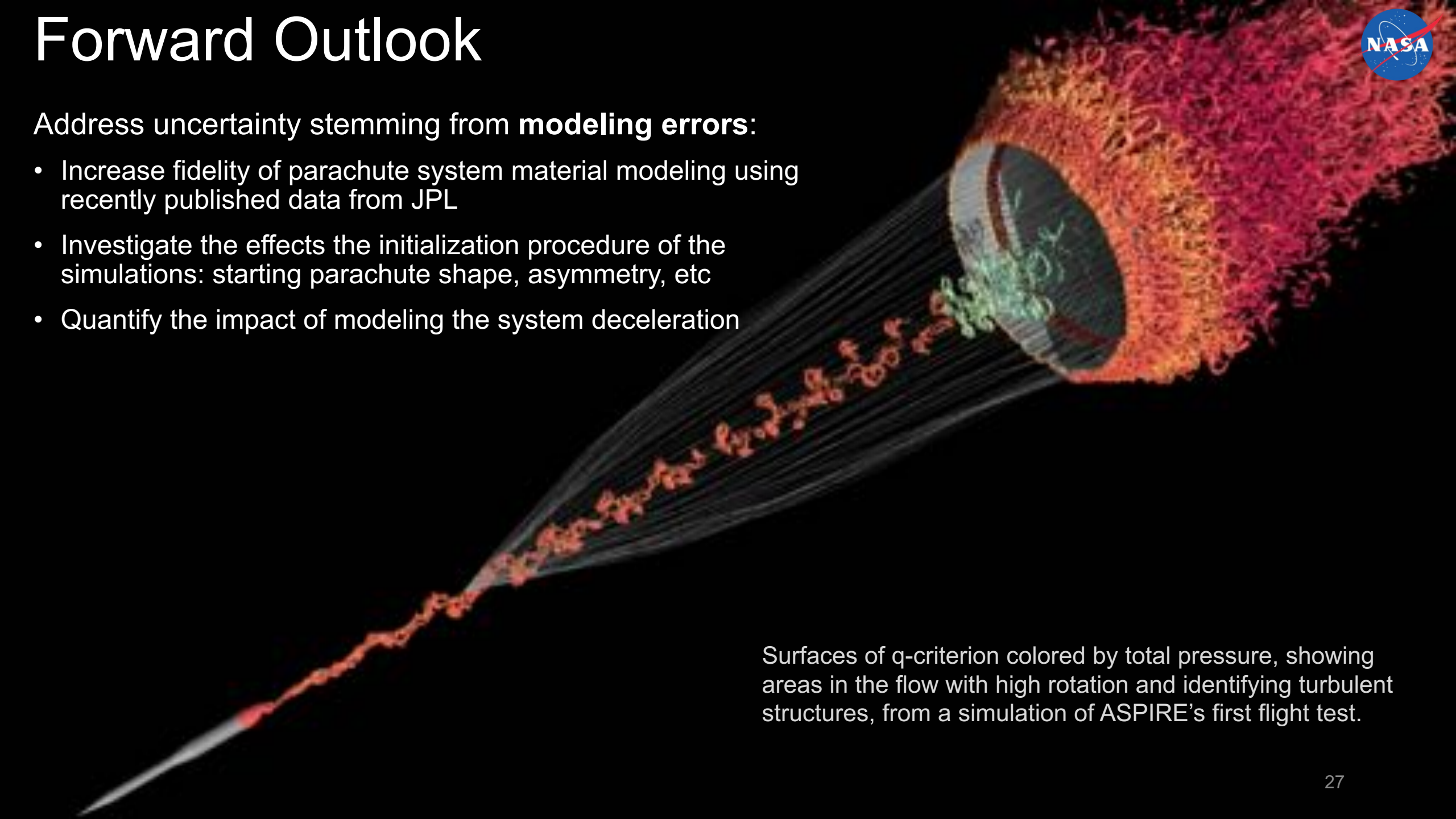
- initial parachute shape: folded accordion shape is not seen in flight test video
- parachute asymmetry: assumed to be perfectly symmetric, causing synchronization of suspension line tension (constructive interference)
- flow initial conditions: parachute loads never reach statistically stationary state in flight test
- parachute material modeling:
  - assumed all gore seams, disk and band leading and trailing edge had very strong Kevlar reinforcements but identical thickness due to lack of information
  - similarly assumed all suspension lines, riser and bridles were made from same material with identical strength and thickness but recently learned that is not a good assumption
- effects of deceleration: the parachute drag causes the whole system to decelerate abruptly during inflation

# Forward Outlook



Address uncertainty stemming from **modeling errors**:

- Increase fidelity of parachute system material modeling using recently published data from JPL
- Investigate the effects the initialization procedure of the simulations: starting parachute shape, asymmetry, etc
- Quantify the impact of modeling the system deceleration

A 3D visualization of a parachute system in flight. The parachute is a large, circular canopy with a complex, textured surface, colored in shades of red, orange, and yellow. It is attached to a smaller, cylindrical component. The flow field around the parachute is depicted with a series of thin, curved lines that represent streamlines or vortices. The background is dark, and the overall scene is illuminated from the side, creating a sense of depth and motion.

Surfaces of  $q$ -criterion colored by total pressure, showing areas in the flow with high rotation and identifying turbulent structures, from a simulation of ASPIRE's first flight test.



# Acknowledgements

- This work is supported by the NASA Entry Systems Modeling (ESM) and the NASA Transformational Tools and Technologies (T<sup>3</sup>) projects
- Computational resources were provided by NASA Advanced Supercomputing (NAS) systems at NASA Ames Research Center

## **Special thanks to:**

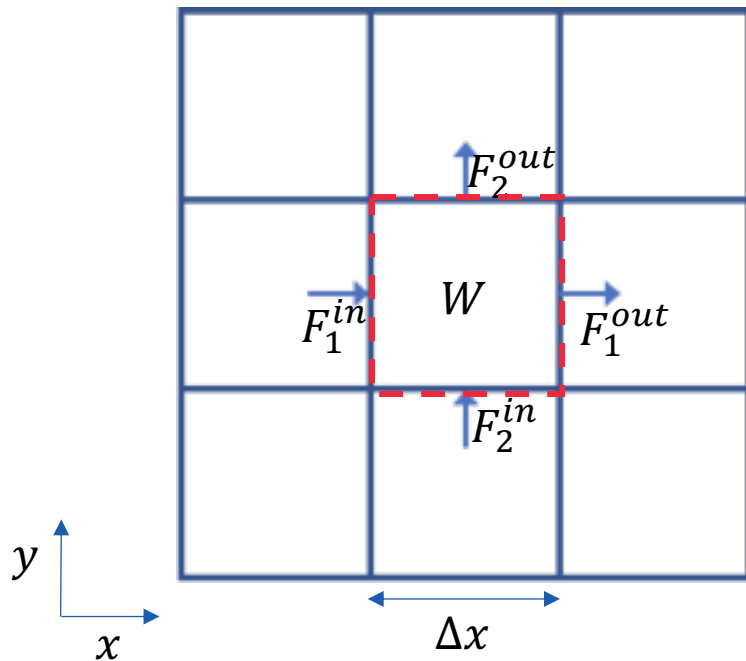
- Jonathan Boustani who developed the geometrically non-linear structural dynamics capability within LAVA, and who performed most of this work
- Gaetan Kenway for helping to improve the parallel efficiency of the structural solver
- Timothy Sandstrom from NASA Ames Research Center for developing and maintaining an interface to the high-performance geometry kernels used in this work
- Michael Barnhardt and Aaron Brandis for insightful discussions on the sources of uncertainty in the ASPIRE flight data and for helping guide the focus of our development efforts



# Backup Slides

# Quick Overview of Unsteady CFD

- Advance conservation of mass, momentum, and energy equations for a gas using fluxes through faces of a control volume (dashed red square) in time from  $t \rightarrow t + \Delta t$  given initial and boundary conditions:



$$\frac{\partial W}{\partial t} = - \frac{\partial F_j}{\partial x_j} \quad W = \begin{bmatrix} \rho \\ \rho u \\ \rho v \\ \rho E \end{bmatrix}$$

$$F_j = \begin{bmatrix} \rho u_j \\ \rho u_1 u_j + p \delta_{1j} \\ \rho u_2 u_j + p \delta_{2j} \\ (\rho E + p) u_j \end{bmatrix}^*$$

$W$ : vector of conserved variables

$F_j$ : flux in  $j$  direction

$\rho$ : density

$u$ : velocity in  $x$  direction

$v$ : velocity in  $y$  direction

$E$ : total energy

$p$ : pressure

$T$ : temperature

$R$ : gas constant

$c_v$ : specific heat at constant volume

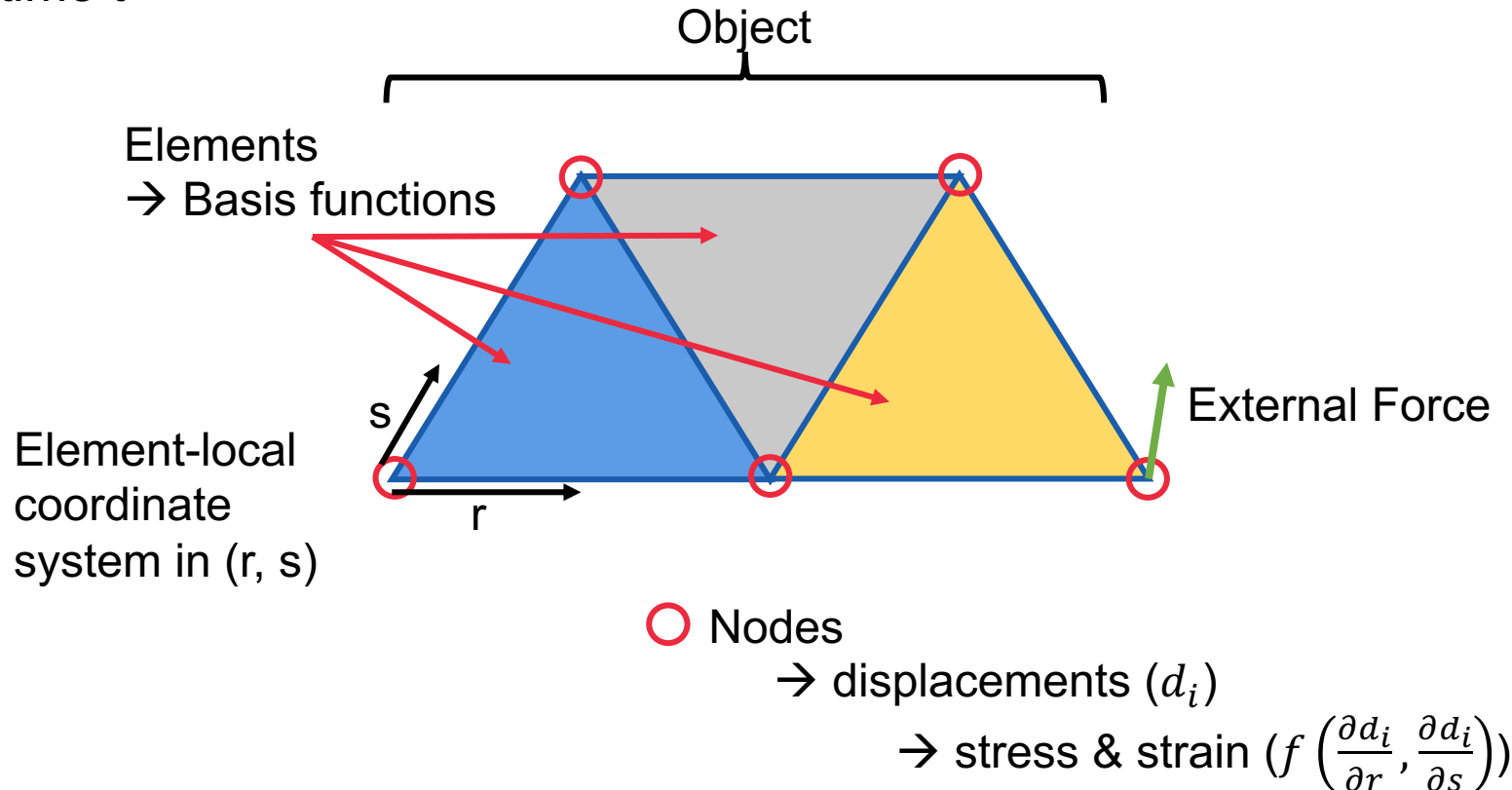
$$p = \rho R T$$

$$E = c_v T + \frac{1}{2} u_i u_i$$

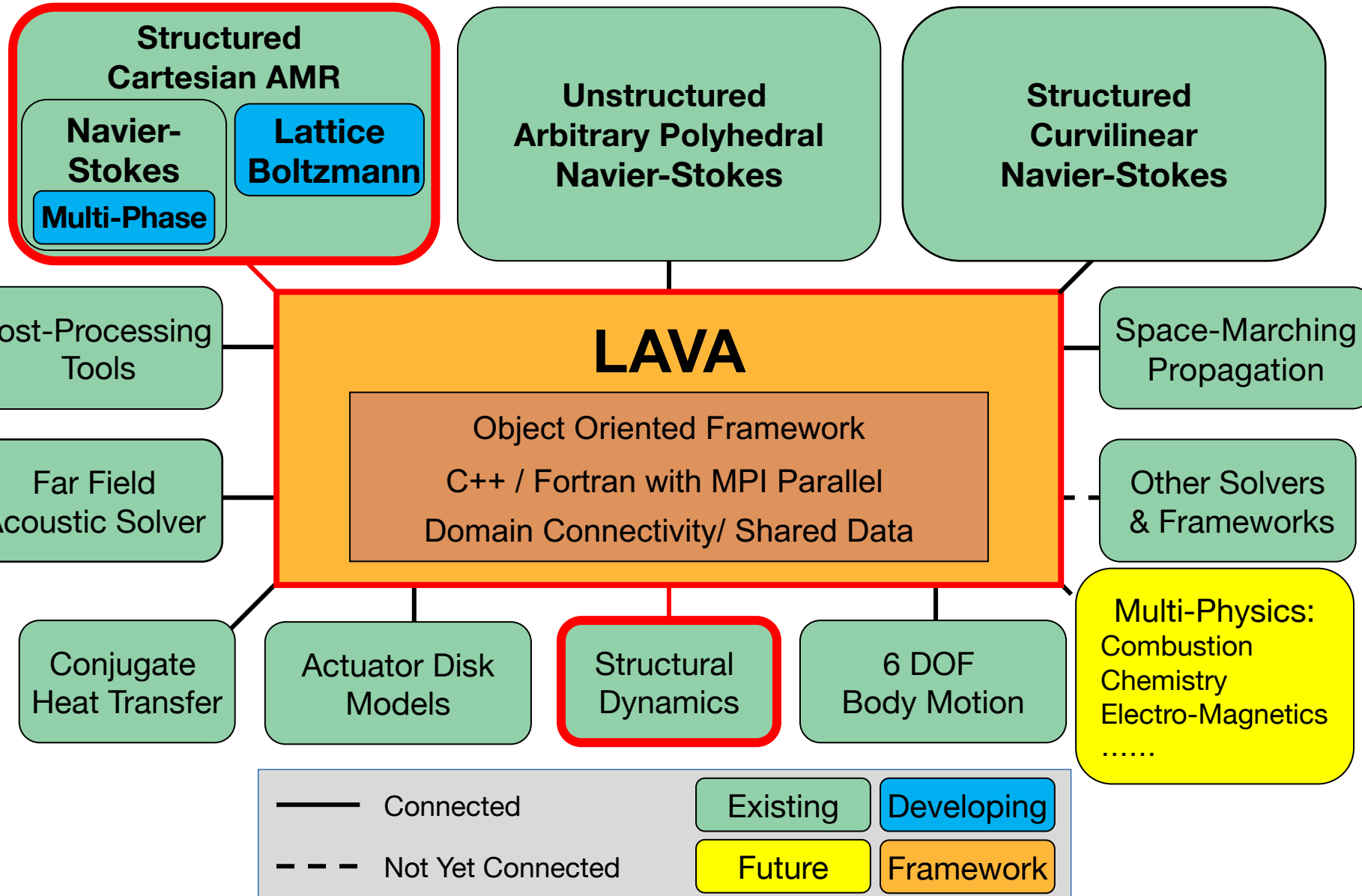
\*Viscous fluxes are neglected for simplicity

# Quick Overview of Unsteady CSD

- Solve the equations of motion of nodes shared across finite elements (e.g. triangles) on an object for their displacements ( $d_i$ ) to reach equilibrium between external forces and internal stresses (functions of gradients of  $d$ ) at time  $t + \Delta t$
- Given the object's material properties (e.g. thickness, density, Young's modulus, Poisson ratio) initial conditions, boundary conditions, and external forces acting on the nodes at time  $t$



# Launch, Ascent and Vehicle Aerodynamics



*Kiris et al. AIAA-2014-0070 & AST-2016*

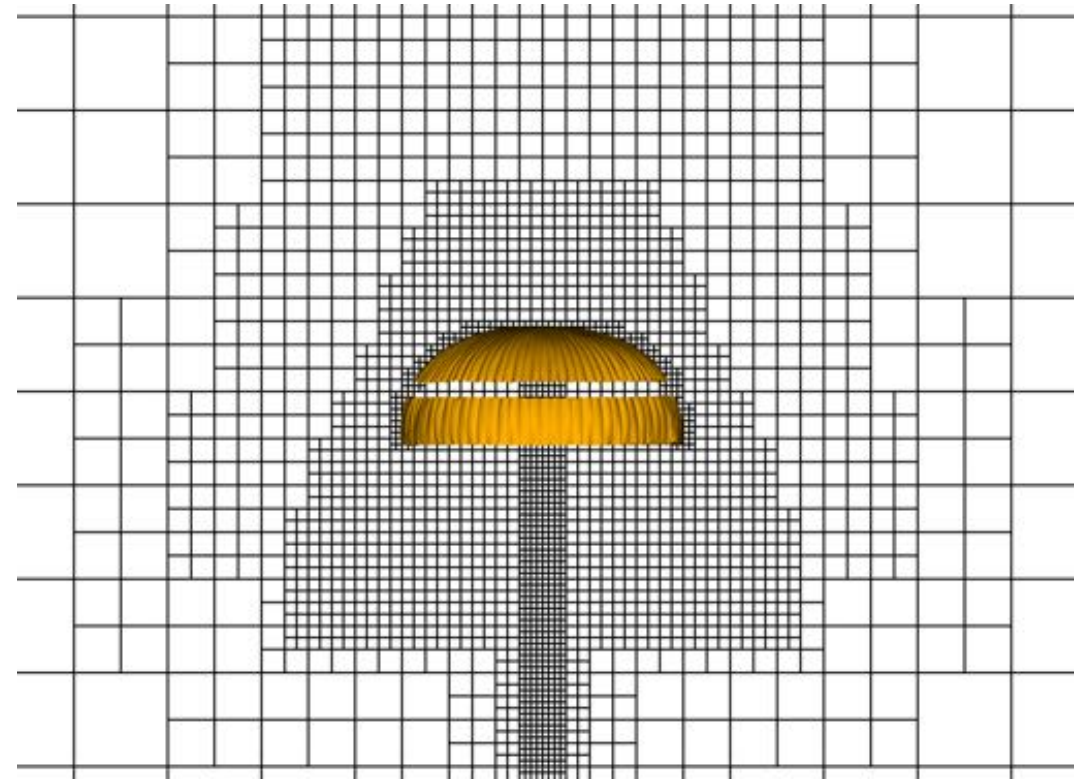
- Other Development Efforts**
- Higher order and low dissipation
  - Curvilinear grid generation
  - Wall modeling
  - LES/DES/ILES Turbulence
  - HEC (optimizations, accelerators, etc)



# CFD Approach For Supersonic Parachute



- Automatically generate octree mesh based on limited user inputs
- Automatically adapt mesh to follow parachute surface as it deforms
- Enforce specific porosity of parachute fabric on oncoming flow with immersed boundary ghost-cell method
- Use explicit Runge-Kutta time integration
- Solve Euler equations with nominally fifth-order accurate shock capturing algorithm (weighted essentially non-oscillatory or WENO)



*Slice of a general Cartesian block structure around an inflated parachute geometry. Each block represents 16x16x16 grid points.*

For more details, please refer to [3]:

[3] Boustani, J., Cadieux, F., Kenway, G. K., Barad, M. F., Kiris, C. C., and Brehm, C., "Fluid-structure interaction simulations of the ASPIRE SR01 supersonic parachute flight test," Aerospace Science and Technology, 2022, p. 107596

# CSD Approach For Supersonic Parachute



- Use geometrically non-linear finite elements with Saint Venant-Kirchhoff hyper-elastic material model to handle parachute's large deformations
- Integrate equations in time using explicit second-order central scheme with high-frequency damping
- Leverage extended MITC3 triangular shell elements with 6 degrees of freedom (DOF) to alleviate shear-locking to model parachute fabric
- Model the suspension lines with Timoshenko beam elements with 6 DOF modified to allow for slack ("can't push on a rope")



*Picture showing parachute structural mesh as it is deformed by a uniform outward pressure in a structural dynamics simulation (decoupled from CFD).*

For more details, please refer to [3] and [4]:

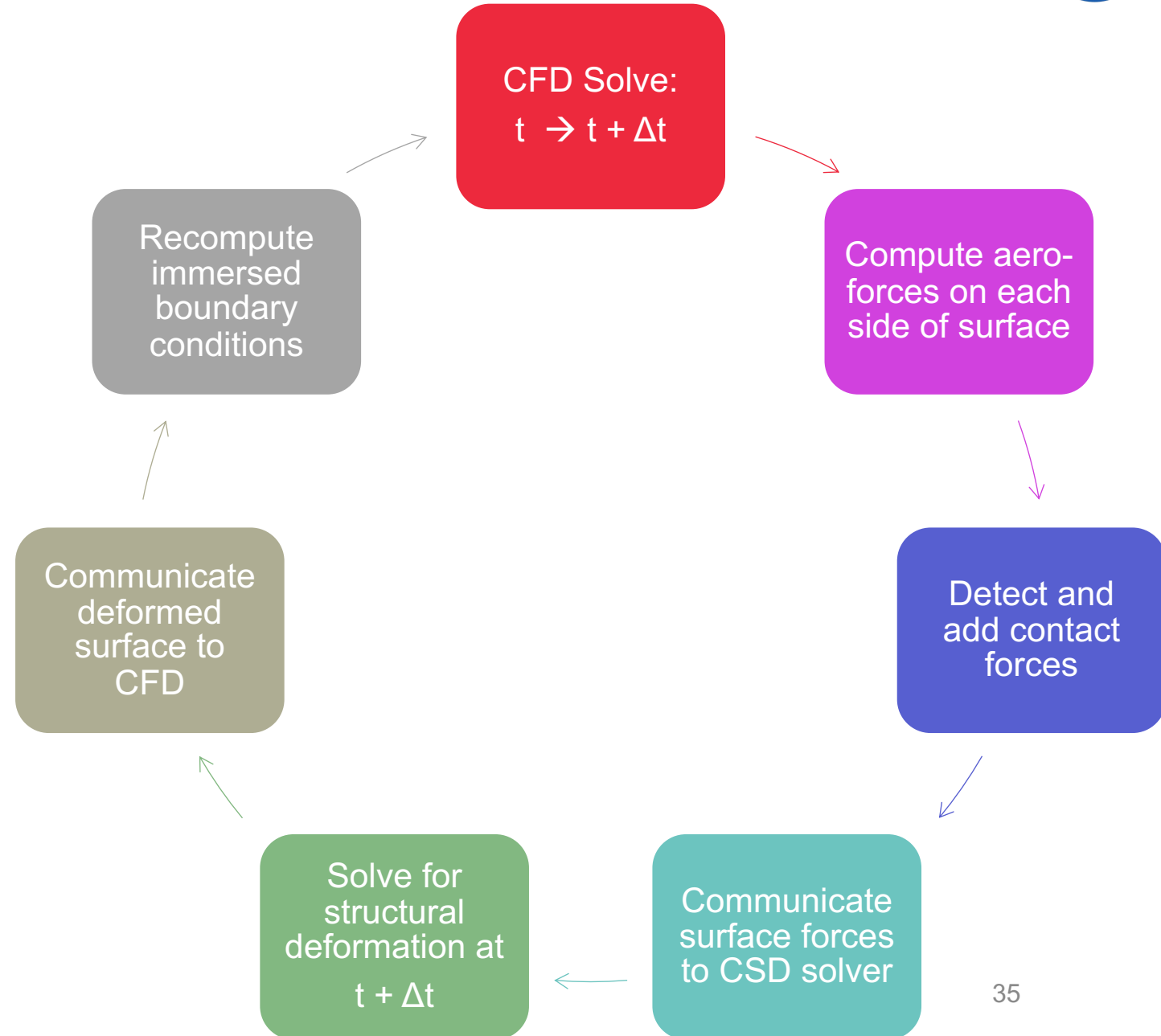
[3] Boustani, J., Cadieux, F., Kenway, G. K., Barad, M. F., Kiris, C. C., and Brehm, C., "Fluid-structure interaction simulations of the ASPIRE SR01 supersonic parachute flight test," *Aerospace Science and Technology*, 2022, p. 107596

[4] Boustani, Jonathan, et al. "Fluid-structure interactions with geometrically nonlinear deformations." *AIAA Scitech 2019 Forum*. 2019

# CFD + CSD Coupling Approach



- Loose-coupling approach
- CFD time advancement limited by Courant–Friedrichs–Lewy (CFL<1) condition
- CSD time advancement is sub-cycled with a smaller  $\Delta t$  to satisfy critical time step if necessary



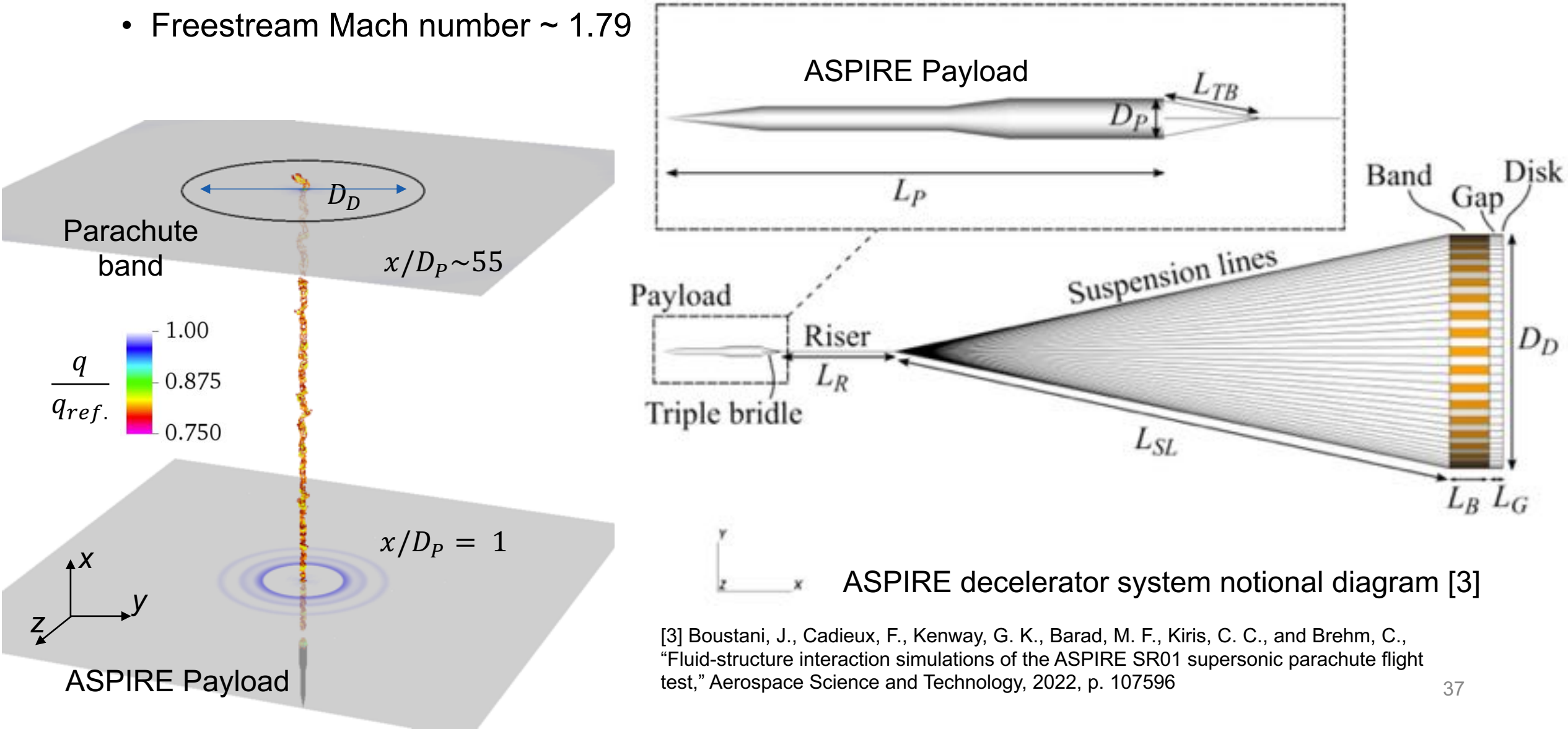


# Core Challenges

- Parachute is made of thin stretchy fabric that go through large deformations → need geometrically non-linear finite element model
- Parachute fabric is porous and does let some air flow through it → need to model porosity
- Parachute is folded into a bag before it is ejected out of the back of the capsule, resulting in lots of self-contact during inflation → need to model contact mechanics
- Parachute is opening in upper atmosphere (low pressure and density environment) and while traveling at supersonic speed → need robust and accurate shock capturing

# ASPIRE Payload Wake

- ASPIRE tests used a slender payload instead of blunt aero-shell like that of Mars 2020
- Freestream Mach number  $\sim 1.79$

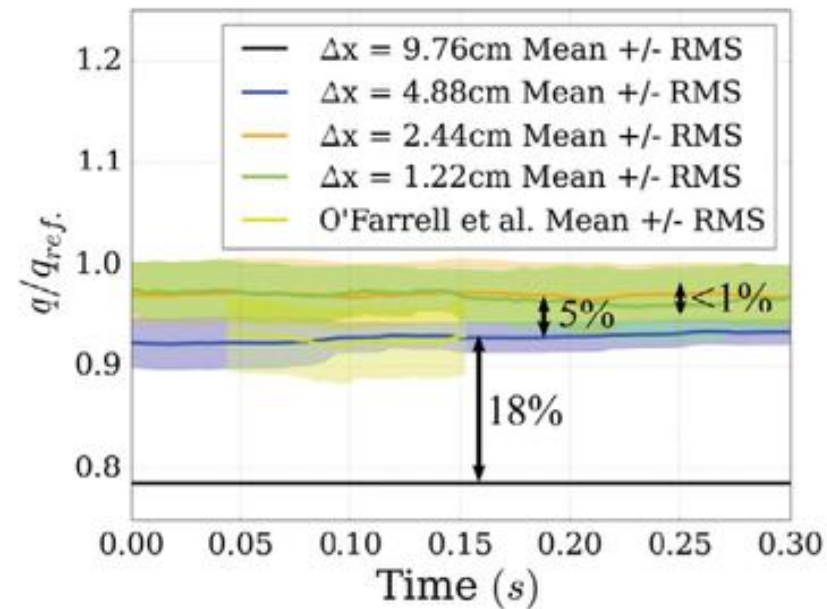


ASPIRE decelerator system notional diagram [3]

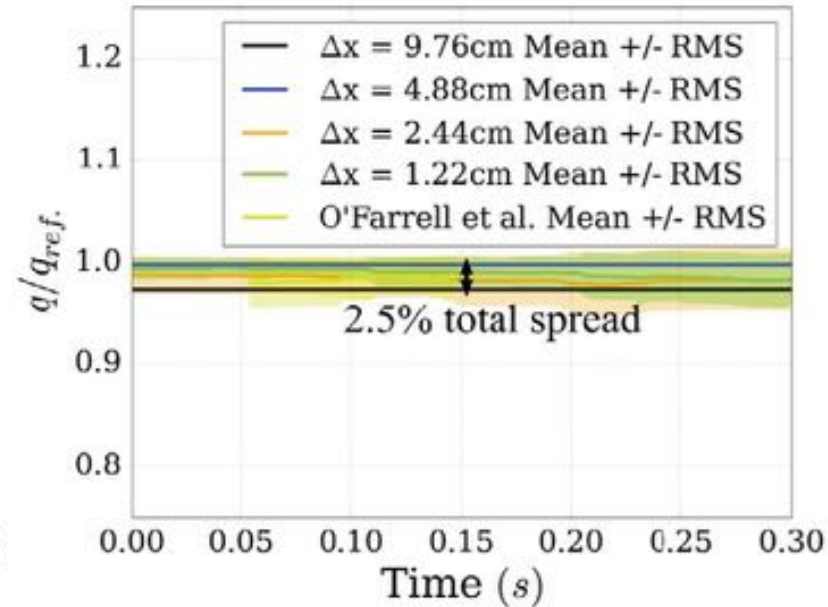
[3] Boustani, J., Cadieux, F., Kenway, G. K., Barad, M. F., Kiris, C. C., and Brehm, C., "Fluid-structure interaction simulations of the ASPIRE SR01 supersonic parachute flight test," Aerospace Science and Technology, 2022, p. 107596

# ASPIRE Payload Wake Deficit

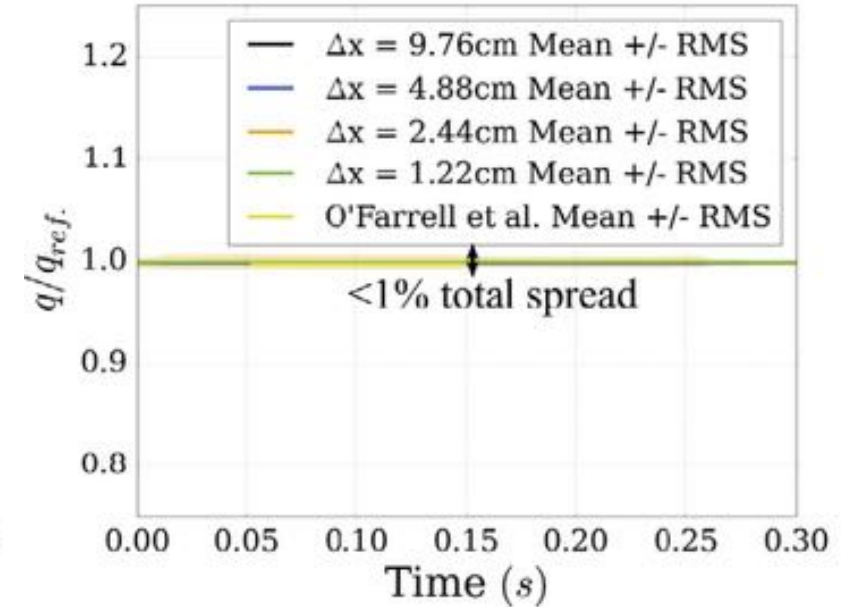
## CFD Grid Convergence Study Results



$$x = 55 D_p, y = 0.5 D_p$$



$$x = 55 D_p, y = D_p$$



$$x = 55 D_p, y = 2 D_p$$

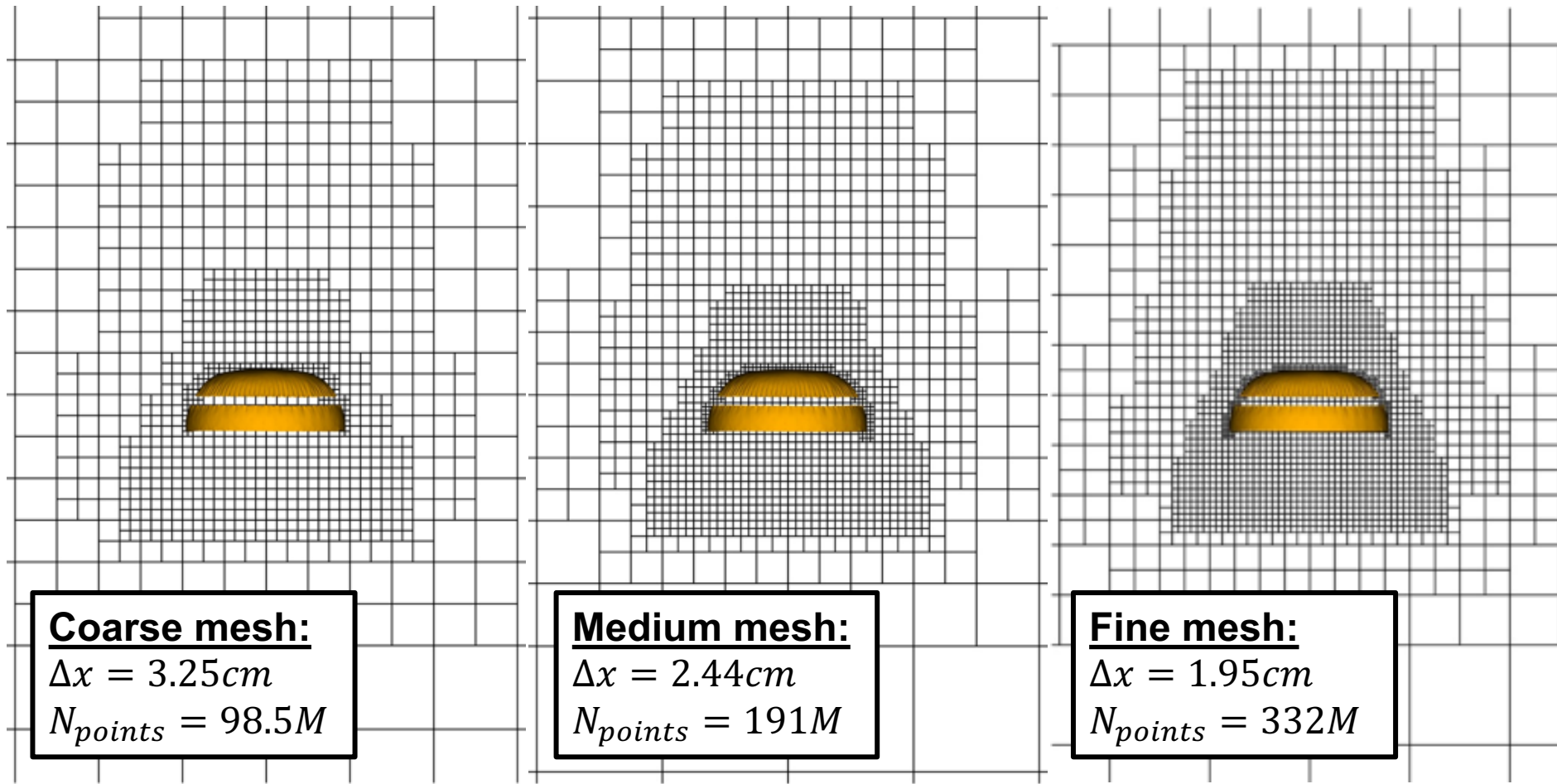
- Wake deficit is minor and very narrow
- < 1% change going from  $\Delta x = 2.44 \text{ cm}$  to  $\Delta x = 1.22 \text{ cm}$
- $\Delta x = 2.44 \text{ cm}$  is sufficient to capture wake deficit

# ASPIRE Inflated Static Canopy

## CFD Grid Convergence Study

Grids are uniformly refined by factors of  $2^{1/3}$  so the total number of cells doubles each time

Same freestream conditions as experience during test when suspension lines first record tension (aka line-stretch event): Mach number  $\sim 1.79$



# ASPIRE Inflated Static Canopy

## CFD Grid Convergence Results

Integrated drag is already converged with  $< 1\%$  difference between all resolutions tested

Only noticeable difference is the level of detail captured in wake turbulence

